Published OnlineFirst August 9, 2011; DOI:10.1158/1055-9965.EPI-11-0400



**Table 1.** Clinicopathologic characteristics of cases in the training ($n = 43$) and validation cohorts (V1: $n = 210$; V2: $n = 113$)

| | Training cohort ($n = 43$) | | | Validation-1 cohort ($n = 210$) | | | Validation-2 cohort ($n = 113$) | | |
|---|---|---|---|---|---|---|---|---|---|
| | Cancer | Healthy | *P* | Cancer | Healthy | *P* | Cancer | Healthy | *P* |
| No. of patients | 22 | 21 | | 101 | 109 | | 26 | 87 | |
| Sex, no. of patients | | | 0.310[a] | | | 0.782[a] | | | 0.252[a] |
| Male | 14 | 17 | | 63 | 70 | | 13 | 56 | |
| Female | 8 | 4 | | 38 | 39 | | 13 | 31 | |
| Age, y | | | <0.001 | | | <0.001 | | | <0.001 |
| Mean (SD) | 62 (12) | 40 (13) | | 64 (11) | 42 (14) | | 63 (12) | 43 (16) | |
| Tumor location | | | *NA* | | | *NA* | | | *NA* |
| Colon | 22 | Ð | | 88 | Ð | | 24 | Ð | |
| Rectum | 0 | Ð | | 13 | Ð | | 2 | Ð | |
| Clinical stage | | | *NA* | | | *NA* | | | *NA* |
| I | 3 | Ð | | 19 | Ð | | 12 | Ð | |
| II | 6 | Ð | | 31 | Ð | | 5 | Ð | |
| III | 8 | Ð | | 32 | Ð | | 8 | Ð | |
| IV | 5 | Ð | | 17 | Ð | | 1 | Ð | |
| Unknown | 0 | Ð | | 2 | Ð | | 0 | Ð | |
| CA19-9 | | | | | | | | | |
| Median, U/mL | 14.7 | 5.5 | 0.010 | 4 | 1.6 | <0.001 | 9.4 | 10.2 | 0.680 |
| >37.0 (ULN), no. of patients | 6 | 2 | | 39 | 5 | | 2 | 4 | |
| CEA | | | | | | | | | |
| Median, ng/mL | 3.5 | 1.7 | 0.002 | 11.8 | 7.6 | 0.001 | 2.6 | 1.7 | 0.008 |
| >5.0 (ULN), no. of patients | 9 | 1 | | 24 | 5 | | 4 | 5 | |
| Total bilirubin | | | | | | | | | |
| Median, mg/dL | 0.4 | 0.5 | 0.114 | 0.4 | 0.5 | <0.001 | 0.4 | 0.5 | <0.001 |
| >1.2 (ULN), no. of patients | 0 | 0 | | 1 | 3 | | 0 | 4 | |
| Adipophilin | | | | | | | | | |
| Mass spectrometry peak intensity[b], mean (SD) | 320 (375) | 96 (78) | <0.001[c] | Ð | Ð | | Ð | Ð | |
| Protein intensity[d], mean (SD) | Ð | Ð | | 3.91 (0.06) | 3.82 (0.13) | <0.001[e] | 3.57 (0.14) | 3.42 (0.20) | <0.001[e] |

NOTE: Wilcoxon test was applied to assess differences between values.
Abbreviations: NA, not applicable; ULN, upper limit of normal.
[a]Calculated by Fisher's exact test.
[b]Intensity of the corresponding peak as measured using quantitative mass spectrometry.
[c]Calculated using Mann–Whitney *U* test.
[d]Measured using reverse-phase protein microarray (logarithmic variable).
[e]Calculated using Welch's *t*-test.

liquid chromatography (NanoFrontier nLC; Hitachi High-technologies) connected to an electrospray ionization quadrupole time-of-flight (ESI-Q-TOF) mass spectrometer (Q-Tof Ultima; Waters).

Mass spectrometry (MS) peaks were detected, normalized, and quantified using the in-house 2DICAL software package, as described previously (13). A serial identification (ID) number was applied to each of the MS peaks detected (1 to 53,009). The stability of liquid chromatography mass spectrometry (LC-MS) was monitored by calculating the correlation coefficient (CC) and coefficient of variance (CV) of every measurement. For all 53,009 peaks observed in the 43 duplicate runs, the mean CC (± SD) was as high as 0.951 (± 0.039) and the mean CV was as low as 0.054 (± 0.011).

### Protein identification by tandem mass spectrometry

Peak lists were generated using the Mass Navigator software package (version 1.2; Mitsui Knowledge Industry) and the peak lists were searched against the SwissProt database (downloaded on April 22, 2009) using the Mascot software package (version 2.2.1; Matrix Science). The search parameters used were as follows: the human protein database was selected; up to 1 missed cleavage was allowed; "none" was designated as the enzyme; mass tolerances for precursor and fragment ions were ± 0.6 and



Downloaded from cebp.aacrjournals.org on October 16, 2011
Copyright © 2011 American Association for Cancer Research

Published OnlineFirst August 9, 2011; DOI:10.1158/1055-9965.EPI-11-0400



± 0.2 Da, respectively; the score threshold was set to $P < 0.05$ on the basis of size of the database used in the search. If a peptide matched multiple proteins, the protein name with the highest Mascot score was selected.

### Immunoblot analysis

Primary antibodies used were mouse monoclonal antibody (mAb) against adipophilin (LifeSpan Biosciences) and mouse mAb against human complement C3b-α (Progen). Ten microliter of 1:50 diluted plasma sample and 0.3 μg of fully recombinant adipophilin (BioVendor) as positive control were separated by SDS-PAGE and electroblotted onto a polyvinylidene difluoride membrane. The membrane was then incubated with primary antibody followed by horseradish peroxidase (HRP)-conjugated anti-mouse IgG as described previously (24, 25). Blots were developed using an enhanced chemiluminescence detection system (GE Healthcare).

### Reverse-phase protein microarray

The plasma samples from the V1 and V2 cohorts were serially diluted 1:32, 1:64, 1:128, and 1:256 using a Biomek 2000 Laboratory Automation Robot (Beckman Coulter), and randomly plotted onto ProteoChip glass slides (Proteogen) in quadruplicate in a 6144-spot/slide format using a Protein Microarrayer Robot (Kaken Geneqs). The spotted slides were incubated overnight with the same primary antibody as used in Western blotting. The slides were incubated with biotinylated anti-mouse IgG (Vector Laboratories) followed by streptavidin–HRP conjugate (GE Healthcare). Peroxidase activity was detected using the Tyramide Signal Amplification Cyanine 5 System (PerkinElmer). The slides were counterstained with Alexa Fluor 546–labeled goat anti-human IgG (Invitrogen; spotting control).

The stained slides were scanned on a microarray scanner (InnoScan 700AL; Innopsys). Fluorescence intensity, determined as mean values of quadruplicate samples, was determined using the Mapix software (Innopsys). All intensity values were transformed into logarithmic variables. The reproducibility of our reverse-phase protein microarray assay was reported previously (18).

### Immunohistochemistry

Twenty colorectal cancer cases were selected from the surgical pathology archive panel of the National Cancer Center Hospital, as described previously (24). Sections (4-μm thick) were cut from paraffin blocks of colorectal cancer tissues and mounted on silanized glass slides and were subsequently stained by the avidin–biotin complex method. The primary antibody was the same as used in immunoblot analysis.

### Statistical analysis

The statistical significance of intergroup differences was assessed with the Wilcoxon test, Mann–Whitney *U* test, Welch's *t* test, Kruskal–Wallis test, or Fisher's exact test, as appropriate. The area under the curve (AUC) value of the receiver operating characteristics (ROC) analysis was calculated for each marker to evaluate its diagnostic significance using ROCKIT software (version 0.9.1; the Kurt Rossmann Laboratories). A composite index of 2 markers was generated using the result of multivariate logistic regression analysis, which also enabled the calculation of sensitivity, specificity, and ROC curves. Statistical analyses were done using an open-source statistical language R (version 2.7.0) with the optional module Design package.

## Results

### Plasma biomarker discovery by quantitative MS

To identify a diagnostic biomarker for patients with colorectal cancer including those with early-stage diseases, we compared the plasma proteomes of 22 colorectal cancer patients with those of 21 healthy controls (training cohort) using 2DICAL (Table 1). Among a total of 53,009 independent MS peaks detected within the range 250 to 1,600 *m/z* and within the time range 20 to 70 minutes, we found 103 peaks with a discriminatory AUC value of >0.800. A representative 2-dimensional view of all the MS peaks, with the *m/z* displayed along the X-axis and the LC retention time (RT) along the Y-axis, is shown in Figure 1A. The 103 MS peaks which distinguished between colorectal cancer patients and healthy controls with AUC values of >0.800 are highlighted in red.

Eleven tandem mass spectrometry spectra acquired from those 103 peaks matched 6 proteins in the database with Mascot score >40 (Supplementary Table S1). We focused attention on a MS peak (ID 83) derived from the amino acid sequence of *ADFP* gene product (Supplementary Fig. S1) because the expression level of adipophilin was previously reported to be upregulated in clear cell renal carcinoma, but no such upregulation has been described in colorectal cancer. The adipophilin-derived MS peak (ID 83, at 749 *m/z* and 47.4 minutes) in representative patients from cancer and control groups is shown in Figure 1B. The distribution of the MS peak (ID 83) in patients with colorectal cancer (red) and healthy controls (blue) in the training cohort (AUC = 0.814) is shown in Figure 1C. The differential expression and identification of adipophilin was confirmed by denaturing SDS-PAGE and immunoblotting analyses (Fig. 1D).

### Protein microarray validation

To further validate the utility of using adipophilin for the diagnosis of colorectal cancer, the relative level of adipophilin in a total of 323 plasma samples was quantified using reverse-phase protein microarrays (Fig. 2). Quadruplicate spots for representative cases with high and low levels of adipophilin are shown in Figure 2. The power of plasma adipophilin level to discriminate colorectal cancer was validated in 2 larger independent validation cohorts (V1: $n = 210$, V2: $n = 113$) that included early-stage colorectal cancer (Table 1). In the V1 cohort, the adipophilin level was significantly higher in patients



Downloaded from cebp.aacrjournals.org on October 16, 2011
Copyright © 2011 American Association for Cancer Research

Published OnlineFirst August 9, 2011; DOI:10.1158/1055-9965.EPI-11-0400



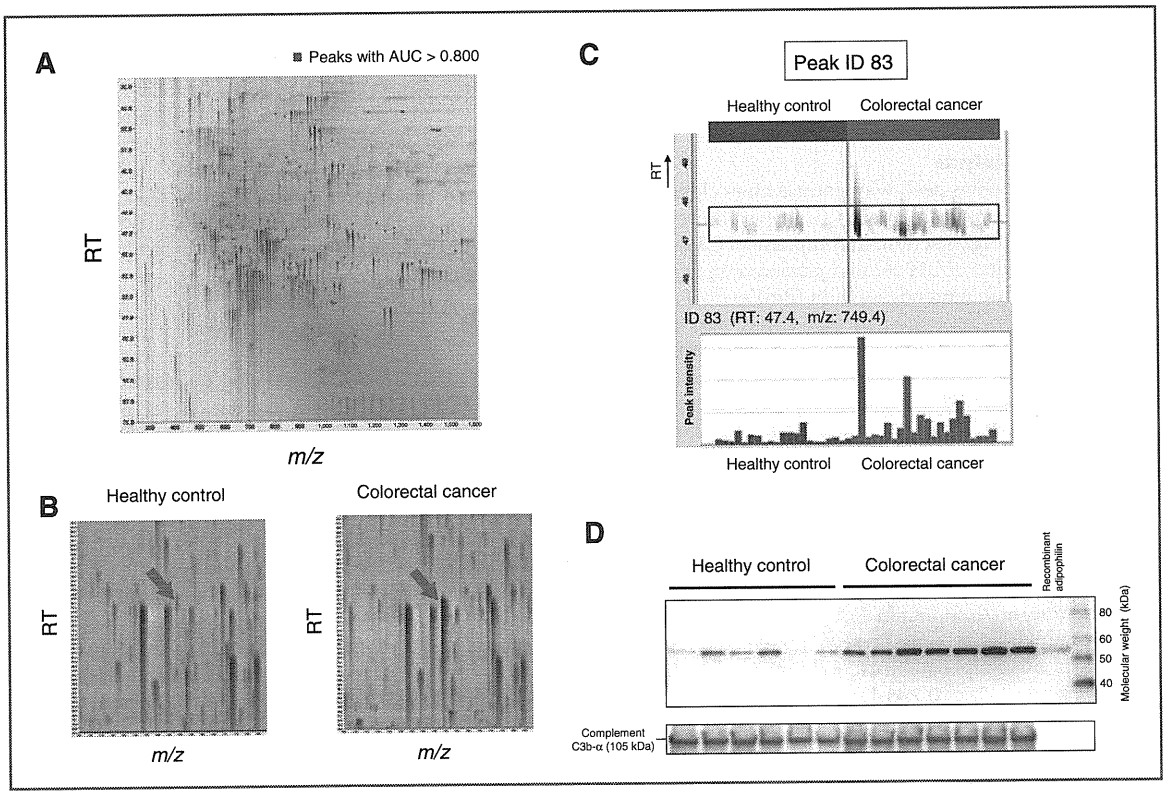


Figure 1. A, two-dimensional display of all (>53,000) MS peaks detected. The 103 MS peaks for which the mean intensity determined in duplicate analyses distinguished between colorectal cancer and healthy control patients (with AUC values >0.800) are highlighted in red. B, adipophilin-derived MS peaks in representative patients from cancer and control groups. Arrows indicate ID 83, at 749 *m/z* and a RT of 47.4 minutes. C, adipophilin-derived MS peaks (ID 83) in 43 duplicate LC-MS runs aligned according to RT (top). Columns represent the mean intensity of duplicate analyses of the 43 individuals in the training cohort (bottom). D, verification of quantitative MS data and protein identification. The levels of plasma adipophilin and complement C3b-α (loading control) were determined using immunoblotting in representative colorectal cancer patients and healthy individuals selected from the training cohort. Recombinant adipophilin (0.3 μg) was applied as a positive control (lane next to the molecular weight standard ladder).

with colorectal cancer than in healthy controls (Welch's *t* test $P = 5.49 \times 10^{-10}$, Fig. 3A and Table 1), with an AUC value of 0.767 (95% CI: 0.699–0.825; Fig. 3B). The colorectal cancer discriminatory power of adipophilin was also apparent in the V2 cohort ($P = 0.00009$, Fig. 3C and Table 1), with an AUC value of 0.742 (95% CI: 0.625–0.836; Fig. 3B).

There was no difference in the plasma level of adipophilin among different disease stages (Kruskal–Wallis test $P = 0.280$). Notably, however, the adipophilin level was significantly higher even in patients with stage I or II disease (localized early colorectal cancer without metastasis to lymph nodes) than in healthy controls, whereas the CEA level in early-stage patients did not significantly differ from that of healthy controls (Table 2).

## Adipophilin complements CEA

The levels of adipophilin and CEA were not mutually correlated (Pearson's $r = 0.13$ in the V1 cohort and 0.12 in the V2 cohort), and the AUC values of CEA in both cohorts (Fig. 3D) were comparable with that of a previous report (26). Combining adipophilin and CEA quantitation yielded a significant improvement in the ability to distinguish patients with colorectal cancer from healthy controls compared with quantitating CEA alone; the AUC improved to 0.849 (95% CI: 0.790–0.896) in the V1 cohort ($P = 0.0008$) and 0.787 (0.673–0.874) in the V2 cohort ($P = 0.022$; Fig. 3D), indicating that plasma adipophilin and CEA have complementary diagnostic utility.

Due to the low prevalence of colorectal cancer among an asymptomatic population, a high specificity is required for a screening biomarker. If we defined the upper limit of the normal range of the composite index (adipophilin plus CEA; Fig. 3D) to include 95% of healthy controls in each validation cohort, the sensitivity of the index was 54% (95% CI: 41–66) in the V1 cohort and 31% (13–56) in the V2 cohort.

## Adipophilin expression in colorectal cancer

The expression and cellular distribution of adipophilin in colorectal cancer tissues were examined using an immunohistochemical assay of 8 well differentiated, 10



Downloaded from cebp.aacrjournals.org on October 16, 2011
Copyright © 2011 American Association for Cancer Research

Published OnlineFirst August 9, 2011; DOI:10.1158/1055-9965.EPI-11-0400



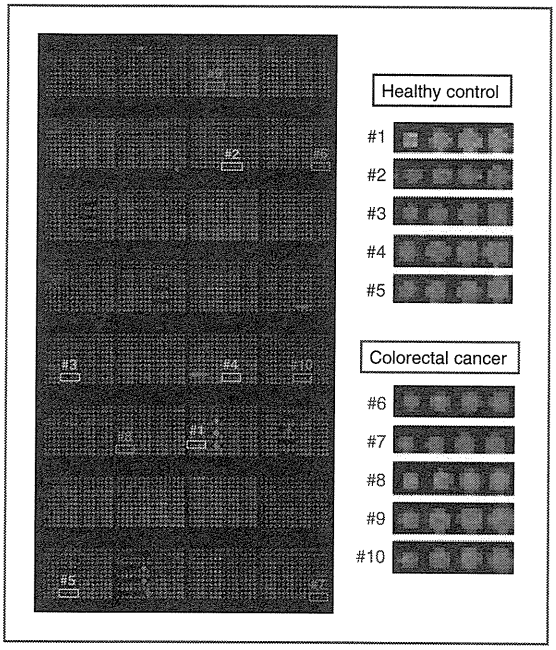


Figure 2. Representative reverse-phase protein microarray slide of the V1 cohort stained with anti-ADFP antibody (left). Magnified images of quadruplicate spots of representative individuals with high and low levels of adipophilin (right).

moderately differentiated, and 2 poorly differentiated adenocarcinomas. A total of 14 of 20 cancer tissues from the well- and moderately differentiated cases showed positive staining for adipophilin, but neither of the 2 poorly differentiated samples was positive. In a majority of the well- and moderately differentiated tumors, strong staining for adipophilin was observed in the cytoplasm or cell membrane of tumor glands facing the basement membrane (Fig. 4A and B). Adipophilin was not expressed in normal epithelial cells of the colorectal mucosa (Fig. 4C). The expression of adipophilin was clearly diminished in cancer cells invading in a scattered manner (Fig. 4D), which is consistent with the lack of staining observed in poorly differentiated tumor samples.

## Discussion

In this study, we first enriched the LMW plasma protein fraction using HFMT, then compared its contents between patients with colorectal cancer and healthy controls using 2DICAL (Fig. 1). The high efficacy of combining HFMT and 2DICAL for plasma biomarker discovery was shown for the first time in our previous study of pancreatic cancer (17), and the present results further strengthened the credible evidence for the applicability of this combination of methods to all types of future plasma biomarker research. Any biomarker candidate identified by proteomic approaches must be validated using a different

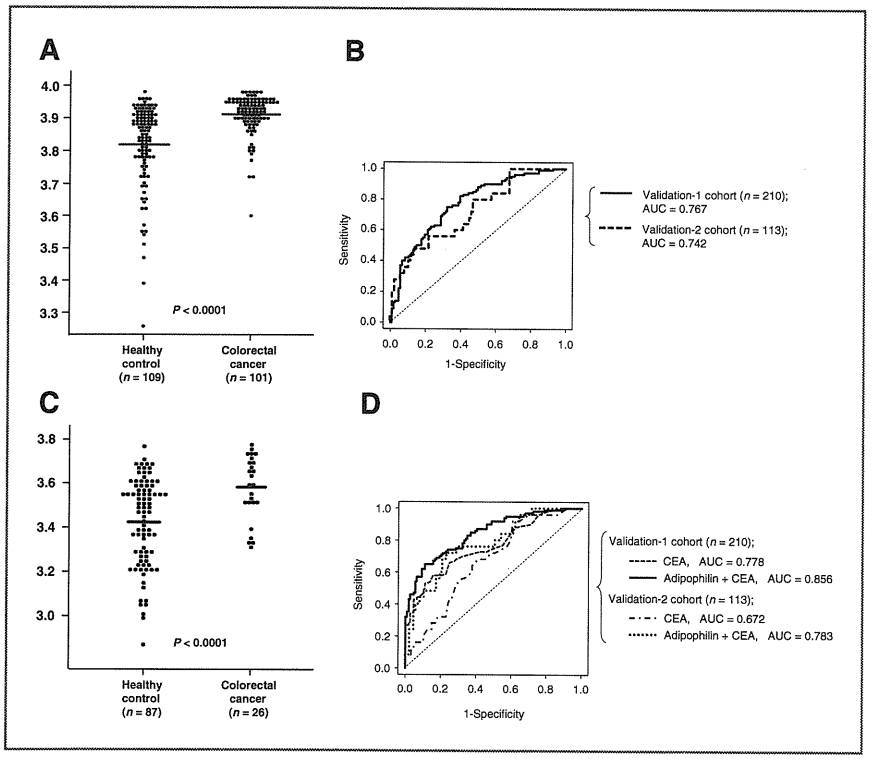


Figure 3. A and C, plasma adipophilin level in healthy controls and patients with colorectal cancer in the V1 (A) and V2 (C) cohorts. Horizontal lines represent the average adipophilin level. B, ROC analyses illustrating the discriminatory capability of adipophilin in the V1 (solid line) and V2 (dashed line) cohorts. D, ROC analyses illustrating the discriminatory value of CEA and the composite index of adipophilin and CEA in the V1 and V2 cohorts.



Downloaded from cebp.aacrjournals.org on October 16, 2011
Copyright © 2011 American Association for Cancer Research

Published OnlineFirst August 9, 2011; DOI:10.1158/1055-9965.EPI-11-0400



**Table 2.** Plasma adipophilin and CEA levels according to clinical stage of colorectal cancer [UICC TNM classification of malignant tumors, 6th edition (2002)] in the V1 cohort

| | Colorectal cancer patients | | | | Healthy controls |
|---|---|---|---|---|---|
| | **Stage I** | **Stage II** | **Stage III** | **Stage IV** | |
| No. of cases | 19 | 31 | 32 | 17 | 109 |
| **Adipophilin[a], mean (SD)** | 3.90 (0.05) | 3.91 (0.07) | 3.91 (0.07) | 3.93 (0.03) | 3.82 (0.13) |
| $P^b$ (vs. healthy controls) | $1.07 \times 10^{-5}$ | $3.31 \times 10^{-6}$ | $1.65 \times 10^{-6}$ | $2.27 \times 10^{-11}$ | Ð |
| **CEA, mean (SD), ng/mL** | 2.63 (1.71) | 13.7 (36.2) | 224 (1,068) | 200 (579) | 2.07 (1.74) |
| $P^b$ (vs. healthy controls) | 0.20 | 0.09 | 0.25 | 0.18 | Ð |

[a]Measured using a reverse-phase protein microarray (values were transformed into logarithmic variables).
[b]Welch's *t* test (comparison with healthy controls).

method in a statistically sufficient number of cases and controls before it can be considered for clinical application. We employed another innovative technology, a reverse-phase protein microarray, for independent validation of our finding that adipophilin discriminates colorectal cancer (Fig. 2). Our high-density protein microarray enabled the high-throughput quantification of 1 protein in hundreds of clinical samples in 1 experiment (18), while keeping the required volume of each sample to a minimum (nanoliter level). Although the availability of clinical samples is often limited, it is often necessary to waste hundreds of microliters of samples for preliminary experiments involving techniques such as conventional ELISA. Because of their minimal sample requirements, plasma microarrays are considered to be ideal alternatives to ELISAs for biomarker validation. However, the absolute concentration and optimal cut-off value of adipophilin were not determined in this study. It may be necessary to establish an ELISA prior to the clinical application of the present results.

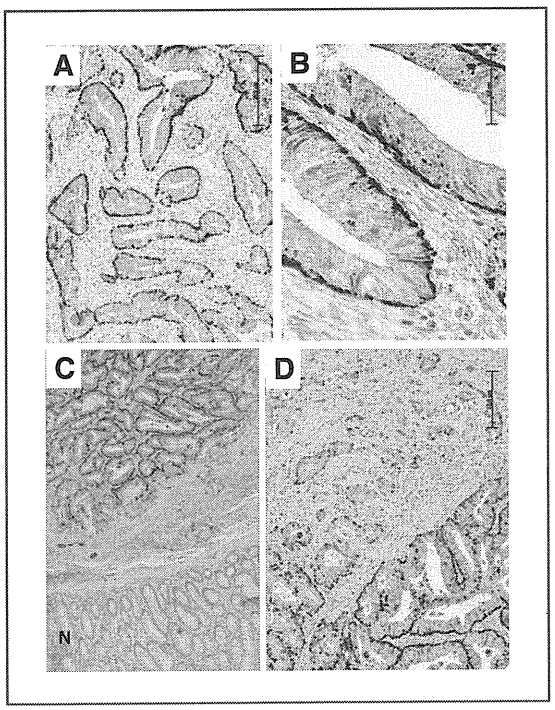


Figure 4. Immunohistochemical analysis of adipophilin in colorectal cancer (A–D) and adjacent normal colonic mucosa (designated by N; C). Original magnification; A and D = 100×; B = 400×; C = 40×.

Although the expression of adipophilin is known to be induced in various types of pathologic and physiologic conditions, such as lactating mammary epithelial cells, few studies have assessed the significance of its expression in cancer cells (27, 28). We found that adipophilin is expressed in well- or moderately differentiated adenocarcinomas, but not in the adjacent normal colonic mucosa or poorly differentiated adenocarcinoma (Fig. 4). The immunohistochemical data suggest that the expression of adipophilin is induced during the process of early colorectal carcinogenesis but lost during the process of cancer promotion. Consistent with our findings, Yao and colleagues also reported that adipophilin expression correlates well with the differentiation status of clear cell renal carcinoma of the kidney (29). They also reported that adipophilin expression is a prognostic factor for the cancer-specific survival of patients with renal clear cell carcinoma (29). The prognostic significance of adipophilin expression in colorectal cancer, however, remains to be determined.

The expression of adipophilin is known to be regulated by hypoxia inducible factor (HIF) and the peroxisome proliferator-activated receptor (PPAR) family of proteins. Both HIF and PPAR were reported to be closely involved in carcinogenesis, especially in colorectal cancer (30, 31). Moreover, PPARγ may be a molecular target of anticancer therapy (32). Because the exact nature of the interactions between these proteins (adipophilin, HIF, and PPAR) has not been extensively investigated, further studies are needed to elucidate the biological and clinicopathologic significance of adipophilin expression in colorectal



Downloaded from cebp.aacrjournals.org on October 16, 2011
Copyright © 2011 American Association for Cancer Research

Published OnlineFirst August 9, 2011; DOI:10.1158/1055-9965.EPI-11-0400



cancer. The present findings may provide novel insights into the molecular mechanism of colorectal cancer development and progression and into the development of new anticancer therapeutics.

There are some limitations to our study. First, we have no data about the body mass index of cases included in this study. The relationship between obesity and an increased risk of colon cancer is now generally accepted (33–35), and alteration of adipocytokine levels can reportedly affect intestinal carcinogenesis (36). Although adipophilin was originally identified as a marker of adipocyte development (27, 37), its relevance to body shape and cachexia remain to be elucidated. Adipophilin is a 50 kDa protein belonging to the PAT family (perilipin, adipophilin, TIP47, S3-12, and OXPAT), which comprises proteins involved in the coating of lipid droplets (27, 38, 39). Second, we have no data of FOB test results for the cases used in this study and thus it was not possible to show the superiority of adipophilin to FOB. However, a recent large-scale study showed that 11% of patients with negative FOB results had cancers or adenomas that required treatment (40). Because the adipophilin level was significantly elevated, even in patients with localized early colorectal cancer (Table 2), adipophilin may supplement or surpass the diagnostic power of FOB. Finally, there was a difference in the age distribution between cancer and control in all cohorts. However, age did not correlate with plasma adipophilin level in the cancer and control group (Pearson's $r = 0.03$ and $r = 0.09$, respectively). We therefore estimate the influence of difference in age to be negligible.

In conclusion, we identified plasma adipophilin as a new tumor marker for colorectal cancer using LMW protein profiling. The increase of plasma adipophilin level in colorectal cancer was validated in 2 larger cohorts, and the diagnostic power was revealed to be superior to that of CEA in the detection of early-stage (stages I and II) colorectal cancer. To our knowledge, this is the first study showing the expression of adipophilin in colorectal cancer. While bearing the above limitations in mind, an independent validation study is warranted.

## Disclosure of Potential Conflicts of Interest

The sponsors of the study had no role in the design of the study, data collection, data analysis and interpretation, the decision to submit the manuscript for publication, or the writing of the manuscript.

## Acknowledgments

We thank Ms. Ayako Igarashi, Ms. Tomoko Umaki, and Ms. Yuka Nakamura for their technical assistance.

## Grant Support

This study was supported by the "Program for Promotion of Fundamental Studies in Health Sciences" conducted by the National Institute of Biomedical Innovation of Japan, the "Third-Term Comprehensive Control Research for Cancer" and "Research on Biological Markers for New Drug Development" conducted by the Ministry of Health and Labor of Japan.

The costs of publication of this article were defrayed in part by the payment of page charges. This article must therefore be hereby marked *advertisement* in accordance with 18 U.S.C. Section 1734 solely to indicate this fact.

Received April 27, 2011; revised July 12, 2011; accepted August 1, 2011; published OnlineFirst August 9, 2011.

## References

1. Jemal A, Siegel R, Ward E, Hao Y, Xu J, Murray T, et al. Cancer statistics, 2008. CA Cancer J Clin 2008;58:71–96.
2. Ministry of Health, Labour and Welfare. Japanese Government: Vital Statistics of Japan. 2009; http://ganjoho.ncc.go.jp/professional/statistics/odjrh3000000hwsa-att/cancer_mortality(1958-2008).xls.
3. Andre T, Boni C, Navarro M, Tabernero J, Hickish T, Topham C, et al. Improved overall survival with oxaliplatin, fluorouracil, and leucovorin as adjuvant treatment in stage II or III colon cancer in the MOSAIC trial. J Clin Oncol 2009;27:3109–16.
4. Wolmark N, Yothers G, O'Connell MJ, Sharif S, Atkins JN, Seay TE, et al. A phase III trial comparing mFOLFOX6 to mFOLFOX6 plus bevacizumab in stage II or III carcinoma of the colon: Results of NSABP Protocol C-08. J Clin Oncol 2009;27: abstr LBA4.
5. Tol J, Koopman M, Cats A, Rodenburg CJ, Creemers GJ, Schrama JG, et al. Chemotherapy, bevacizumab, and cetuximab in metastatic colorectal cancer. N Engl J Med 2009;360:563–72.
6. Mandel JS, Bond JH, Church TR, Snover DC, Bradley GM, Schuman LM, et al. Reducing mortality from colorectal cancer by screening for fecal occult blood. Minnesota Colon Cancer Control Study. N Engl J Med 1993;328:1365–71.
7. Kronborg O, Fenger C, Olsen J, Jorgensen OD, Sondergaard O. Randomised study of screening for colorectal cancer with faecal-occult-blood test. Lancet 1996;348:1467–71.
8. Hardcastle JD, Chamberlain JO, Robinson MH, Moss SM, Amar SS, Balfour TW, et al. Randomised controlled trial of faecal-occult-blood screening for colorectal cancer. Lancet 1996;348:1472–7.
9. Greenberg PD, Bertario L, Gnauck R, Kronborg O, Hardcastle JD, Epstein MS, et al. A prospective multicenter evaluation of new fecal occult blood tests in patients undergoing colonoscopy. Am J Gastroenterol 2000;95:1331–8.
10. van Rossum LG, van Rijn AF, Laheij RJ, van Oijen MG, Fockens P, van Krieken HH, et al. Random comparison of guaiac and immunochemical fecal occult blood tests for colorectal cancer in a screening population. Gastroenterology 2008;135:82–90.
11. Locker GY, Hamilton S, Harris J, Jessup JM, Kemeny N, Macdonald JS, et al. ASCO 2006 update of recommendations for the use of tumor markers in gastrointestinal cancer. J Clin Oncol 2006;24:5313–27.
12. Yamaguchi U, Nakayama R, Honda K, Ichikawa H, Hasegawa T, Shitashige M, et al. Distinct gene expression-defined classes of gastrointestinal stromal tumor. J Clin Oncol 2008;26:4100–8.
13. Ono M, Shitashige M, Honda K, Isobe T, Kuwabara H, Matsuzuki H, et al. Label-free quantitative proteomics using large peptide data sets generated by nanoflow liquid chromatography and mass spectrometry. Mol Cell Proteomics 2006;5:1338–47.
14. Matsubara J, Ono M, Negishi A, Ueno H, Okusaka T, Furuse J, et al. Identification of a predictive biomarker for hematologic toxicities of gemcitabine. J Clin Oncol 2009;27:2261–8.
15. Negishi A, Ono M, Handa Y, Kato H, Yamashita K, Honda K, et al. Large-scale quantitative clinical proteomics by label-free liquid chromatography and mass spectrometry. Cancer Sci 2009;100:514–9.
16. Ono M, Matsubara J, Honda K, Sakuma T, Hashiguchi T, Nose H, et al. Prolyl 4-hydroxylation of alpha-fibrinogen: a novel protein modification revealed by plasma proteomics. J Biol Chem 2009;284:29041–9.
17. Matsubara J, Honda K, Ono M, Tanaka Y, Kobayashi M, Jung G, et al. Reduced plasma level of CXC chemokine ligand 7 in patients with



Downloaded from cebp.aacrjournals.org on October 16, 2011
Copyright © 2011 American Association for Cancer Research

Published OnlineFirst August 9, 2011; DOI:10.1158/1055-9965.EPI-11-0400



pancreatic cancer. Cancer Epidemiol Biomarkers Prev 2011;20:160–71.
18. Matsubara J, Ono M, Honda K, Negishi A, Ueno H, Okusaka T, et al. Survival prediction for pancreatic cancer patients receiving gemcitabine treatment. Mol Cell Proteomics 2010;9:695–704.
19. Kennedy S. The role of proteomics in toxicology: identification of biomarkers of toxicity by protein expression analysis. Biomarkers 2002;7:269–90.
20. Tirumalai RS, Chan KC, Prieto DA, Issaq HJ, Conrads TP, Veenstra TD. Characterization of the low molecular weight human serum proteome. Mol Cell Proteomics 2003;2:1096–103.
21. Anderson NL, Anderson NG. The human plasma proteome: history, character, and diagnostic prospects. Mol Cell Proteomics 2002;1:845–67.
22. Tanaka Y, Akiyama H, Kuroda T, Jung G, Tanahashi K, Sugaya H, et al. A novel approach and protocol for discovering extremely low-abundance proteins in serum. Proteomics 2006;6:4845–55.
23. http://www.fhcrc.org/science/international_biomarker/.
24. Honda K, Yamada T, Hayashida Y, Idogawa M, Sato S, Hasegawa F, et al. Actinin-4 increases cell motility and promotes lymph node metastasis of colorectal cancer. Gastroenterology 2005;128:51–62.
25. Idogawa M, Yamada T, Honda K, Sato S, Imai K, Hirohashi S. Poly (ADP-ribose) polymerase-1 is a component of the oncogenic T-cell factor-4/beta-catenin complex. Gastroenterology 2005;128:1919–36.
26. Carpelan-Holmstrom M, Louhimo J, Stenman UH, Alfthan H, Jarvinen H, Haglund C. Estimating the probability of cancer with several tumor markers in patients with colorectal disease. Oncology 2004;66:296–302.
27. Heid HW, Moll R, Schwetlick I, Rackwitz HR, Keenan TW. Adipophilin is a specific marker of lipid accumulation in diverse cell types and diseases. Cell Tissue Res 1998;294:309–21.
28. de Wilde J, Smit E, Snepvangers FJ, de Wit NW, Mohren R, Hulshof MF, et al. Adipophilin protein expression in muscle–a possible protective role against insulin resistance. FEBS J 2010;277:761–73.
29. Yao M, Huang Y, Shioi K, Hattori K, Murakami T, Nakaigawa N, et al. Expression of adipose differentiation-related protein: a predictor of cancer-specific survival in clear cell renal carcinoma. Clin Cancer Res 2007;13:152–60.
30. Paul SA, Simons JW, Mabjeesh NJ. HIF at the crossroads between ischemia and carcinogenesis. J Cell Physiol 2004;200:20–30.
31. Osawa E, Nakajima A, Wada K, Ishimine S, Fujisawa N, Kawamori T, et al. Peroxisome proliferator-activated receptor gamma ligands suppress colon carcinogenesis induced by azoxymethane in mice. Gastroenterology 2003;124:361–7.
32. Grommes C, Landreth GE, Heneka MT. Antineoplastic effects of peroxisome proliferator-activated receptor gamma agonists. Lancet Oncol 2004;5:419–29.
33. Pischon T, Lahmann PH, Boeing H, Friedenreich C, Norat T, Tjonneland A, et al. Body size and risk of colon and rectal cancer in the European Prospective Investigation Into Cancer and Nutrition (EPIC). J Natl Cancer Inst 2006;98:920–31.
34. Giovannucci E, Michaud D. The role of obesity and related metabolic disturbances in cancers of the colon, prostate, and pancreas. Gastroenterology 2007;132:2208–25.
35. Renehan AG, Tyson M, Egger M, Heller RF, Zwahlen M. Body-mass index and incidence of cancer: a systematic review and meta-analysis of prospective observational studies. Lancet 2008;371:569–78.
36. Mutoh M, Teraoka N, Takasu S, Takahashi M, Onuma K, Yamamoto M, et al. Loss of adiponectin promotes intestinal carcinogenesis in Min and wild-type mice. Gastroenterology 2011;140:2000–8.
37. Brasaemle DL. Thematic review series: adipocyte biology. The perilipin family of structural lipid droplet proteins: stabilization of lipid droplets and control of lipolysis. J Lipid Res 2007;48:2547–59.
38. Jiang HP, Serrero G. Isolation and characterization of a full-length cDNA coding for an adipose differentiation-related protein. Proc Natl Acad Sci U S A 1992;89:7856–60.
39. Martin S, Parton RG. Lipid droplets: a unified view of a dynamic organelle. Nat Rev Mol Cell Biol 2006;7:373–8.
40. Johnson CD, Chen MH, Toledano AY, Heiken JP, Dachman A, Kuo MD, et al. Accuracy of CT colonography for detection of large adenomas and cancers. N Engl J Med 2008;359:1207–17.



Downloaded from cebp.aacrjournals.org on October 16, 2011
Copyright © 2011 American Association for Cancer Research

Journal of proteome research

ARTICLE

pubs.acs.org/jpr

# Peptidomics-Based Discovery of an Antimicrobial Peptide Derived from Insulin-Like Growth Factor-Binding Protein 5

Tsukasa Osaki, Kazuki Sasaki,* and Naoto Minamino*

Department of Molecular Pharmacology, National Cerebral and Cardiovascular Center Research Institute, Suita, Osaka 565-8565, Japan

Supporting Information

**ABSTRACT:** Antimicrobial peptides (AMPs) are effector molecules that are able to kill or inactivate microbial pathogens. However, most AMPs harbor multiple basic amino acids that hamper current proteomic identification. In our peptidomic survey of endogenous peptides, we identified a novel intramolecular disulfide-linked 22-residue amidated peptide. This peptide, designated AMP-IBP5 (antimicrobial peptide derived from insulin-like growth factor-binding protein 5), showed antimicrobial activity against six of the eight microorganisms tested at concentrations comparable to or lower than those for well-characterized AMPs cathelicidin and β-defensin-2. AMP-IBP5 is identical at the amino acid level between human, mouse, rat, pig, and cow. Natural occurrence of this peptide as the originally isolated form was demonstrated in the rat brain and intestine, using mass spectrometric characterization of major immunoreactivity. The peptide is flanked N-terminally by a single arginine and C-terminally by a common amidation signal, indicating that insulin-like growth factor-binding protein 5 (IGFBP-5) undergoes specific cleavage by a defined set of processing proteases. Furthermore, the intramolecular linkage C199-C210 reveals itself as a correct disulfide pairing in the precursor protein, the finding not inferred from closely related family members IGFBP-4 and -6. In principle, neither conventional proteomics nor bioinformatics would achieve the identification of this AMP. Our study exemplifies the impact of peptidomics to study naturally occurring peptides.

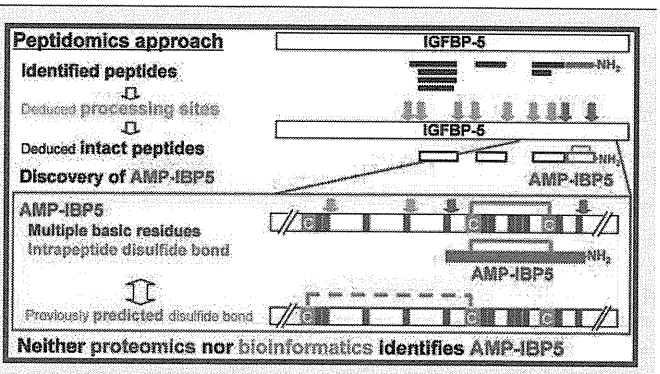


**KEYWORDS:** antimicrobial peptide, bioactive peptide, insulin-like growth factor-binding protein 5, mass spectrometry, peptidomics, proteolytic processing, secretopeptidome

## INTRODUCTION

Bioactive peptides, such as peptide hormones and antimicrobial peptides (AMPs), have been identified through activity-guided biochemical purification that starts with a bulk of biological samples. Recently, technological advances in mass spectrometry (MS) enable us to identify naturally occurring peptides present in mixtures.[1−3] Nevertheless, we are faced with a daunting task of identifying bioactive peptides of a secretory nature owing to their relative low abundance. Once extracted from biological samples, secreted peptides are not discriminated from nonsecreted peptides or peptide fragments caused by degradation of cytosolic proteins. Since relatively abundant molecules are preferentially detected in MS schemes, we need to work on samples rich in secreted peptides for facilitating the discovery of bioactive peptides. We recently used tandem mass spectrometry (MS/MS) techniques to characterize a total pool of naturally occurring peptides that are released by exocytosis from cells in culture. This study, referred to as secretopeptidome analysis, allows us to identify peptides localized in secretory granules in a noninvasive as well as efficient manner.[4,5]

In the present study, we focused on secreted peptides with a highly basic nature. Some bioactive peptides, especially AMPs, harbor multiple basic amino acids. In fact, well-characterized mammalian AMPs β-defensin-2[6] and cathelicidin[7] both bear a net charge of +6 at pH 7.0. These peptides should be analyzed in their native forms, and therefore cannot be studied by current proteomics that needs an enzymatic digestion step for MS-based identification. We characterized highly basic fractions of the secretopeptidome from cultured human pancreatic neuroendocrine tumor cells and identified a previously unknown peptide that arises from insulin-like growth factor-binding protein 5 (IGFBP-5). With regard to antimicrobial activity and spectrum, this peptide is almost as potent as cathelicidin and even superior to β-defensin-2. The peptide was thus designated AMP-IBP5 (antimicrobial peptide derived from IGFBP-5). We provide evidence that AMP-IBP5 is generated through site-specific cleavages in the brain and small intestine. In addition, the identification of this intramolecular disulfide-linked peptide led us to conclude that IGFBP-5 protein possesses a disulfide pairing different from that previously predicted on the basis of analogy to IGFBP-4 and -6.[8] While bioinformatics is currently used for in silico prediction of bioactive peptides, this peptide could not be identified in a

**Received:** November 5, 2010
**Published:** January 06, 2011

ACS Publications © 2011 American Chemical Society

situation where we had relied on the previous incorrect disulfide pairing. Our data demonstrated that peptidomics is a promising tool to uncover previously uncharacterized peptides.

## EXPERIMENTAL PROCEDURES

### Peptide Preparation

Monolayer cultures of the human pancreatic neuroendocrine tumor cell line QGP-1[9] were rinsed three times with Hanks' medium (Invitrogen, Carlsbad, CA). Culture supernatant of the cells (ca. $3.2 \times 10^7$ cells) stimulated with 10 $\mu$M forskolin and 10 $\mu$M carbachol for 15 min was harvested. Peptides were extracted and gel-filtrated as previously described.[4] Cysteine residues of the gel-filtrated samples were converted to carbamidomethyl cysteines (CmC) using dithiothreitol and iodoacetamide, followed by desalting and lyophilization. Resultant products were dissolved in solvent A (10 mM ammonium formate, pH 3.8: acetonitrile (ACN) = 9:1 (v/v)) and applied to a TSK gel SP-2SW cation-exchange column (1.0 × 50 mm; TOSOH, Tokyo, Japan) equilibrated with solvent A, and eluted at a flow rate of 50 $\mu$L/min with a gradient of 0−100% solvent B (1 M ammonium formate, pH 3.8: ACN = 9:1 (v/v)) in 30 min and then maintained at 100% B for 20 min. Highly basic fractions eluted after 30 min and the preceding fractions eluted between 0 and 30 min were separately desalted and applied to a C18 PepMap column (0.075 × 150 mm; Dionex, Sunnyvale, CA) using an Ultimate liquid chromatography (LC) system (Dionex) equilibrated with solvent A (5% ACN, 0.1% trifluoroacetic acid (TFA)) at a flow rate of 300 nL/min. Peptides were eluted with four steps, 5% B (95% ACN, 0.1% TFA) in 5 min, a linear gradient of 5−60% B in 55 min, a linear gradient of 60−100% B in 5 min, and then 100% B in 20 min. Fractions were collected every 20 s from 10 min after sample injection and spotted onto a 384-well matrix-assisted laser desorption/ionization (MALDI) plate with an infusion of 1.75 mg/mL α-cyano-4-hydroxy cinnamic acid (Nacalai tesque, Kyoto, Japan) in 50% ACN, 0.1% TFA at a flow rate of 1.5 $\mu$L/min using a Probot microfraction collector (Dionex).

### MS Analysis

Samples spotted on a MALDI plate were analyzed on a MALDI-TOF/TOF mass spectrometer (4800 Proteomics Analyzer, Applied Biosystems, Foster City, CA). Each spot was first analyzed in MS positive ion reflector mode in the mass range from 1000 to 5000 Da by accumulating signals of 1000 laser shots. The 15 most abundant parent ions with a signal-to-noise ratio >20 were selected for top-down MS/MS scans, excluding identical parent ions contained in adjacent spots from a given LC-MALDI run. MS/MS was conducted using medium collision energy in positive ion mode.

### Data Analysis and Peptide Identification

Peak lists were generated by the "Launch Peaks to Mascot" function of 4000 Series Explorer software (ver. 3.5, Applied Biosystems) using the default parameters supplied by the manufacturer. Peak lists were searched against IPI Human (80128 entries on June 18, 2009) using Mascot (ver. 2.2), with no enzyme specification. Carbamidomethylation of cysteine was set as a fixed modification, and pyroglutamination and C-terminal amidation were simultaneously allowed as variable modifications. Peptide tolerance was set to 125 ppm and MS/MS tolerance was 0.4 Da. The significance threshold was the Mascot default setting of 5%. In Tables 1 and 2, peptides with a score above the identity threshold (corresponding to an expectation value below 0.05) were listed and considered identified.

### Peptide Synthesis

Peptides derived from IGFBP-5 were synthesized on an Abacus peptide synthesizer (Sigma Genosys, Sigma Aldrich Japan, Hokkaido, Japan) using Fmoc (*N*-(9-fluorenyl) methoxycarbonyl) strategy, purified by reverse phase high performance liquid chromatography (HPLC), and verified for correct synthesis by MS and amino acid analysis. Purity of the peptides was confirmed on separate HPLC systems.

### Heparin-Binding Assay

Synthetic peptides (1 nmol) were dissolved in 450 $\mu$L of phosphate-buffered saline (PBS, 10 mM phosphate buffer, pH 7.0 containing 0.15 M NaCl) and incubated with 50 $\mu$L of heparin-Sepharose CL-6B (GE Healthcare, Piscataway, NJ) at room temperature for 1 h. Supernatant was obtained by centrifugation at 800 × g for 3 min. Beads were washed three times with PBS (1 mL each). All the supernatants were combined as unbound fraction. After washing, bound peptides were eluted off the beads in 1 mL of 20 mM Tris-HCl, pH 8.0, containing 1.5 M NaCl (bound fractions). One-tenth volume of the bound and unbound fractions was each subjected to a reverse phase HPLC system. The linear gradient consisted of 10−60% ACN in 0.1% TFA for 40 min at a flow rate of 0.05 mL/min on a C18 reverse phase HPLC column (Vydac 218TP5115, 1.0 × 150 mm; Hesperia, CA). For a positive control of heparin-binding activity, cathelicidin (LL37; Bachem, Bubendorf, Switzerland) was used.[10]

### Measurement of Antibacterial and Antifungal Activity

AlamarBlue (BioSource International, Camarillo, CA) was used to determine antimicrobial activity. As a consequence of bacterial growth, this redox indicator turns from blue to red in color. Antimicrobial activities of test peptides (up to 10 $\mu$M) or IGFBP-5 protein (1 $\mu$M; Ray Biotech, Norcross, GA) were assessed for the target microbes *Enterococcus hirae* (*E. hirae*), *Micrococcus luteus* (*M. luteus*), *Staphylococcus aureus* (*S. aureus*) 209P, *S. saprophyticus* KD, *Escherichia coli* (*E. coli*) B, *E. coli* K12, *E. coli* kp and *Pichia pastoris* (*P. pastoris*) GS115. The optimal growth temperature of *M. luteus*, *S. saprophyticus* KD and *P. pastoris* GS115 was 30 °C and that of the other microbes was 37 °C. After grown in 3% tryptosoy broth (Eiken Chemical, Tokyo, Japan) for 16 h with shaking at each optimal temperature, cells were washed twice with 10 mM phosphate buffer, pH 7.0, and diluted to $8 \times 10^5$ colony-forming units/ml in the same buffer. Twenty-five microliters of bacteria suspension was mixed with an equal volume of sample in the absence or presence of peptides, and incubated for 1 h. After incubation, 200 $\mu$L of 3% tryptosoy broth containing 10% alamarBlue was added to the reaction mixture and further incubated as follows: 4 h for *E. hirae*, *S. aureus* 209P and *E. coli* B; 6 h for *E. coli* K12 and *E. coli* kp; 7 h for *M. luteus*; 7.5 h for *S. saprophyticus* KD; and 20 h for *P. pastoris* GS115. Aliquots containing all assay reagents but microbes were used as blank. After incubation, the reactions were monitored by absorbance at 570 and 600 nm. Molar extinction coefficients of $OD_{570}$ and $OD_{600}$ in the oxidative condition are 80586 and 117216. Therefore, viability (%) was expressed using the following formula: viability (%) = (117216 × $OD_{570}$ − 80586 × $OD_{600}$ in the presence of peptides/117216 × $OD_{570}$ − 80586 × $OD_{600}$ in the absence of peptides) × 100. The classical colony formation assay was also performed as described[11,12] using *S. aureus* 209P, *E. coli* K12 and *P. pastoris* GS115. For positive controls of

**Table 1. Peptides Identified in Highly Basic Fractions**[a]

| precursor | IPI accession | $m/z$ (obsd) | $M_r$ (calc) (Da) | mass error (Da) | MASCOT score | expect. | N-term | peptide | C-term | net charge (pH 7.0) |
|---|---|---|---|---|---|---|---|---|---|---|
| CgA | 00383975 | 1779.87 | 1778.93 | −0.07 | 63 | 0.026 | L | SFRARAYGFRGPGPQL | R | +3 |
| CgB | 00006601 | 2460.91 | 2460.12 | −0.21 | 125 | $6.90 \times 10^{-9}$ | M | AHGYGEESEEERGLEPGKGRHH | R | −3 |
| CgB | 00006601 | 1995.79 | 1994.94 | −0.16 | 83 | 0.00018 | R | FLGEGHHRVQENQMDKA | R | −1 |
| CgB | 00006601 | 1952.87 | 1952.03 | −0.17 | 65 | 0.0044 | R | GLEPGKGRHHRGRGGEPR | A | +3 |
| CgB | 00006601 | 2106.84 | 2105.98 | −0.15 | 59 | 0.011 | R | SETHAAGHSQEKTHSREKS | S | −1 |
| CGRP | 00027855 | 2390.12 | 2389.32 | −0.21 | 98 | $9.70 \times 10^{-6}$ | G | LLSRSGGVVKNNFVPTNVGSKAF-NH2 | G | +4 |
| CT | 00000914 | 2435.85 | 2435.07 | −0.23 | 69 | 0.0013 | R | DMSSDLERDHRPHVSMPQNAN | C-term | −2 |
| DSG2 | 00028931 | 1822.88 | 1822.03 | −0.16 | 99 | $1.70 \times 10^{-6}$ | R | NENKLLPKHPHLVRQ | K | +2 |
| IGFBP5 | 00029236 | 2770.21 | 2769.44 | −0.24 | 61 | 0.046 | R | AVYLPNCDRKGFYKRKQCKPSR-NH2 | G | +7 |
| NUCB1 | 00893068 | 1580.70 | 1579.85 | −0.16 | 72 | 0.0031 | R | ELDFVSHHVRTKL | D | 0 |
| PC2 | 00643663 | 3111.38 | 3110.55 | −0.18 | 73 | 0.0031 | R | <QVAAEHGFGVRKLPFAEGLYHFYHNGLA | K | −1 |
| PC2 | 00643663 | 2423.07 | 2422.24 | −0.18 | 116 | $3.20 \times 10^{-8}$ | A | ERPVFTNHFLVELHKGGEDKA | R | −1 |
| PC2 | 00643663 | 1976.90 | 1975.99 | −0.10 | 109 | $7.20 \times 10^{-7}$ | R | KLPFAEGLYHFYHNGLA | K | 0 |
| PC2 | 00643663 | 1390.57 | 1389.71 | −0.15 | 71 | 0.0037 | R | SLHHKQQLERD | P | −1 |
| PC2 | 00643663 | 1643.71 | 1642.87 | −0.16 | 87 | $9.30 \times 10^{-5}$ | R | SLHHKQQLERDPR | V | +1 |
| SST | 00000130 | 1157.44 | 1156.55 | −0.11 | 70 | 0.0024 | K | AGCKNFFWK | T | +2 |
| SST | 00000130 | 1258.48 | 1257.60 | −0.12 | 67 | 0.0054 | K | AGCKNFFWKT | F | +2 |
| SST | 00000130 | 1593.64 | 1592.74 | −0.11 | 59 | 0.043 | K | AGCKNFFWKTFTS | C | +2 |
| SST | 00000130 | 1753.62 | 1752.78 | −0.17 | 77 | $7.10 \times 10^{-5}$ | K | AGCKNFFWKT FTSC | C-term | +2 |
| SST | 00000130 | 1625.61 | 1624.72 | −0.11 | 86 | $6.40 \times 10^{-5}$ | G | CKNFFWKTFTSC | C-term | +2 |
| SST | 00000130 | 1334.54 | 1333.63 | 0.10 | 74 | 0.0016 | A | GCKNFFWKTF | T | +2 |
| SST | 00000130 | 1682.63 | 1681.74 | −0.12 | 91 | $1.90 \times 10^{-5}$ | A | GCKNFFWKTFTSC | C-term | +2 |
| VGF | 00289501 | 3706.59 | 3705.83 | −0.25 | 69 | 0.0071 | R | AQEEAEAEERRLQEQEELENYIEHVLLRRP | C-term | −6 |
| VGF | 00289501 | 1786.80 | 1785.90 | −0.11 | 70 | 0.0062 | H | HALPPSRHYPGREAQA | R | +1 |
| VGF | 00289501 | 1724.74 | 1723.87 | −0.13 | 70 | 0.0052 | Y | HHALPPSRHYPGREA | Q | +1 |
| VGF | 00289501 | 1923.82 | 1922.96 | −0.15 | 88 | $1.80 \times 10^{-5}$ | Y | HHALPPSRHYPGREAQA | R | +1 |
| VGF | 00289501 | 1351.55 | 1350.67 | −0.13 | 68 | 0.0065 | R | HYHHALPPSRH | Y | +1 |
| VGF | 00289501 | 1953.80 | 1952.95 | −0.16 | 53 | 0.05 | R | HYHHALPPSRHYPGRE | A | +1 |
| VGF | 00289501 | 2024.81 | 2023.99 | −0.18 | 89 | $1.10 \times 10^{-5}$ | R | HYHHALPPSRHYPGREA | Q | +1 |
| VGF | 00289501 | 2152.91 | 2152.05 | −0.15 | 88 | $1.60 \times 10^{-5}$ | R | HYHHALPPSRHYPGREAQ | A | +1 |
| VGF | 00289501 | 2223.91 | 2223.08 | −0.18 | 94 | $4.20 \times 10^{-6}$ | R | HYHHALPPSRHYPGREAQA | R | +1 |
| VGF | 00289501 | 1610.68 | 1609.80 | −0.13 | 69 | 0.0052 | R | HYHHALPPSRHYP-NH2 | G | +2 |
| VGF | 00289501 | 2380.01 | 2379.18 | −0.18 | 54 | 0.043 | R | RHYH HALPPSRHYPGREAQA | R | +2 |
| VGF | 00289501 | 1766.75 | 1765.90 | −0.16 | 79 | 0.00065 | R | RHYHHALPPSRHYP-NH2 | G | +3 |
| VGF | 00289501 | 2564.15 | 2563.35 | −0.21 | 121 | $9.50 \times 10^{-9}$ | R | RLQEQEELENYIEHVLLRRP | C-term | −2 |
| VGF | 00289501 | 1594.76 | 1593.89 | −0.14 | 66 | 0.014 | R | TLQPPSALRRRHY | H | +3 |
| VGF | 00289501 | 2086.87 | 2086.02 | −0.16 | 68 | 0.008 | H | YHHALPPSRHYPGREAQA | R | 0 |

[a] Peptides whose expectation values (Expect., column 7) were less than 0.05 are listed. $M_r$ (calc) represents the theoretical monoisotopic molecular mass (Da) of the peptide sequence. MASCOT scores are indicated in column 6. The N-terminal (N-term) and C-terminal (C-term) flanking one amino acid (columns 8 and 10) are shown. Net charge (pH 7.0) was calculated as follows: D and E are −1, K and R are +1, and H is 0. N-terminal amino group is +1, and C-terminal carboxyl group is −1. <Q, pyroglutamic acid; -NH2, C-terminal amidation. CgA, chromogranin A; CgB, chromogranin B; CGRP, calcitonin gene-related peptide; CT, calcitonin; DSG2, desmoglein 2; IGFBP5, insulin-like growth factor-binding protein 5; NUCB1, nucleobindin 1; PC2, prohormone convertase 2; SST, somatostatin.


1872
dx.doi.org/10.1021/pr101114a |J. Proteome Res. 2011, 10, 1870–1880

Table 2. IGFBP-5-Derived Peptides Identified by Mass Spectrometry[a]

| m/z (obsd) | $M_r$ (calc) (Da) | mass error (Da) | MASCOT score | identity threshold | expect. | N-term | peptide | C-term |
|---|---|---|---|---|---|---|---|---|
| 3332.62 | 3331.54 | 0.07 | 134 | 54 | $5.50 \times 10^{-10}$ | VKIER | DSREHEEPTTSEMAEETYSPKIFRPKH | RISEL |
| 2974.46 | 2973.38 | 0.07 | 165 | 54 | $4.10 \times 10^{-13}$ | ERDSR | EHEEPTTSEMAEETYSPKIFRPKHT | RISEL |
| 2956.13 | 2955.37 | −0.25 | 154 | 57 | $1.10 \times 10^{-11}$ | ERDSR | <EHEEPTTSEMAEETYSPKIFRPKHT | RISEL |
| 2873.41 | 2872.33 | 0.07 | 80 | 54 | 0.00013 | ERDSR | EHEEPTTSEMAEETYSPKIFRPKH | TRISE |
| 1812.88 | 1811.93 | −0.05 | 143 | 54 | $7.80 \times 10^{-11}$ | DRRKK | LTQSKFVGGAENTAHPR | IISAP |
| 2080.34 | 2079.07 | 0.26 | 71 | 50 | 0.0005 | GPCRR | HMEASLQELKASPRMVPR | AVYLP |
| 1596.80 | 1595.81 | −0.01 | 72 | 54 | 0.00097 | GPCRR | HMEASLQELKASPR | MVPRA |
| 2770.21 | 2769.44 | −0.24 | 61 | 60 | 0.046 | RMVPR | AVYLPNCDRKGFYKRKQCKPSR-NH2 | GRKRG |

[a] Peptides whose MASCOT scores (column 4) exceeded identity thresholds (column 5) are listed. Mr (calc) represents the theoretical monoisotopic molecular mass (Da) of the peptide sequence. Expectation values (Expect.) are indicated in column 6. The N-terminal (N-term) and C-terminal (C-term) flanking five amino acid sequences (columns 7 and 9) are shown. <E, pyroglutamic acid; -NH2, C-terminal amidation.

antimicrobial activity, cathelicidin and β-defensin-2 (Peptide Institute, Osaka, Japan) were used.

### Statistical Analysis

Statistical analysis was performed using Student's $t$ test, with a level of significance set at $p < 0.05$.

### Preparation of Cell Culture Supernatant

The culture supernatant from QGP-1 was prepared as described above. Monolayer culture of the human lung neuroendocrine tumor cell line SHP-77[13] (Ca. $1.1 \times 10^7$ cells) was stimulated with 50 mM potassium chloride and 10 μM carbachol for 10 min and its culture supernatant was harvested. Peptides were extracted as previously described[4] and used for radioimmunoassay (RIA).

### Tissue Collection from Sprague-Dawley Rats

All experimental procedures of tissue collection from rats and immunization of rabbits were approved by our institutional animal experiments and care committee. Brain, pituitary gland, lung, heart, stomach, small intestine, liver, pancreas, kidney and uterus were collected from three female Sprague-Dawley rats (11-week-old, 220−280 g) immediately after decapitation, and used for RIA.

### Antibody Preparation

Synthetic AMP-IBP5 (AVYLPNCDRKGFYKRKQCKPSR-$NH_2$, intramolecularly disulfide-linked) was conjugated with bovine thyroglobulin (Sigma Aldrich, St. Louis, MO) by the action of water-soluble carbodiimide (Peptide Institute). Rabbits were immunized with each conjugate emulsified with an equal volume of Freund's complete adjuvant as reported.[14]

### RIA

RIA was carried out as reported[15] using intramolecularly disulfide-linked $^{125}$I-radiolabeled YAVYLPNCDRKGFYKRKQCKP SR-$NH_2$ and anti-AMP-IBP5 antibody (#569-5) at a dilution of 1:210 000. A fifty percent inhibitory concentration ($IC_{50}$) of ligand binding in the RIA was 20 fmol/tube. Specificity of the RIA was examined with C-terminally Gly-extended AMP-IBP5, carbamidomethylated (CAM)-AMP-IBP5, IGFBP-5 protein and seven known bioactive peptides, vasopressin, calcitonin, adrenomedullin, proadrenomedullin N-terminal 20-amino acid peptide (PAMP-20), neurokinin A, angiotensin II and leucine-enkephalin. The six bioactive peptides except PAMP-20 showed no cross-reactivity up to 100 000 fmol/tube, and IGFBP-5 protein had no cross-reactivity up to 10 000 fmol/tube. The $IC_{50}$ values of C-terminally Gly-extended AMP-IBP5, CAM-AMP-IBP5, and PAMP-20 (arginine amide) were 20 000, 20, and 100 000 fmol/tube, respectively. These results indicate that the antiserum strictly recognizes the C-terminal region including amide structure but not the disulfide bond or the intact IGFBP-5 protein.

### Immunological Detection of AMP-IBP5

Tissues were collected as described above, extracted and condensed with a Sep-Pak C18 cartridge as described previously.[16] An aliquot of cartridge eluate was examined by RIA to quantify immunoreactive (IR)-AMP-IBP5. Brain and small intestine extracts were loaded onto a gel filtration column (Sephadex G-50 fine, GE Healthcare; 1.8 × 135 cm) equilibrated with 1 M $CH_3COOH$ at a flow rate of 7 mL/h, fractionated every 6 mL/tube, and assessed by RIA to evaluate an IR-AMP-IBP5 level in each fraction. Fractions containing most abundant IR-AMP-IBP5 were pooled, lyophilized, and separated on a reverse phase HPLC column (Symmetry300 C18 5 μ, 4.6 × 250 mm; Waters Co., Milford, MA) equilibrated with solvent A (10% ACN, 0.1% TFA) at a flow rate of 1 mL/min. Adsorbed samples were eluted with a linear gradient of 0−100% B (60% ACN, 0.1% TFA) in 60 min, fractionated every 1 mL/tube, and assessed by RIA.

For MS of immunoprecipitates, the fraction containing a highest level of IR-AMP-IBP5 in the reverse phase HPLC was lyophilized, dissolved in 40 μL of the antibody (#569-5) 10-fold diluted with PBS, and incubated overnight with 10 μL of Protein A-Sepharose CL-4B (GE Healthcare) at 4 °C. Immunocomplexes were washed three times with PBS and twice with distilled water (1 mL each), followed by elution in 20 μL of 1% TFA and desalting using u-C18 Zip Tips (Millipore, Billerica, MA). Recovered AMP-IBP5-IR materials were spotted on target plates with α-cyano-4-hydroxy cinnamic acid matrix and then analyzed in MS positive ion reflector mode in the mass range from 1000 to 5000 Da on a 4800 Proteomics Analyzer.

### SDS-PAGE and Immunoblotting

Tissues were collected as described above and extracted with 10 volumes (w/v) of SDS-PAGE loading buffer, followed by separation on a 15% SDS-PAGE gel and transfer to a PVDF membrane (GE Healthcare) as reported.[17] Membranes were probed with the first antibody and then probed with horseradish peroxidase-conjugated goat antirabbit IgG (1:5000; Cell Signaling Technology, Beverly, MA). First antibodies were used as follows: a rabbit polyclonal antibody (H-100) raised against human IGFBP-5[81-180] (1:1000; Santa Cruz Biotechnology, Santa Cruz, CA) for detecting intact IGFBP-5; and a rabbit monoclonal antibody (14C10) raised against human/rat glyceraldehyde 3-phosphate dehydrogenase (GAPDH) (1:5000; Cell

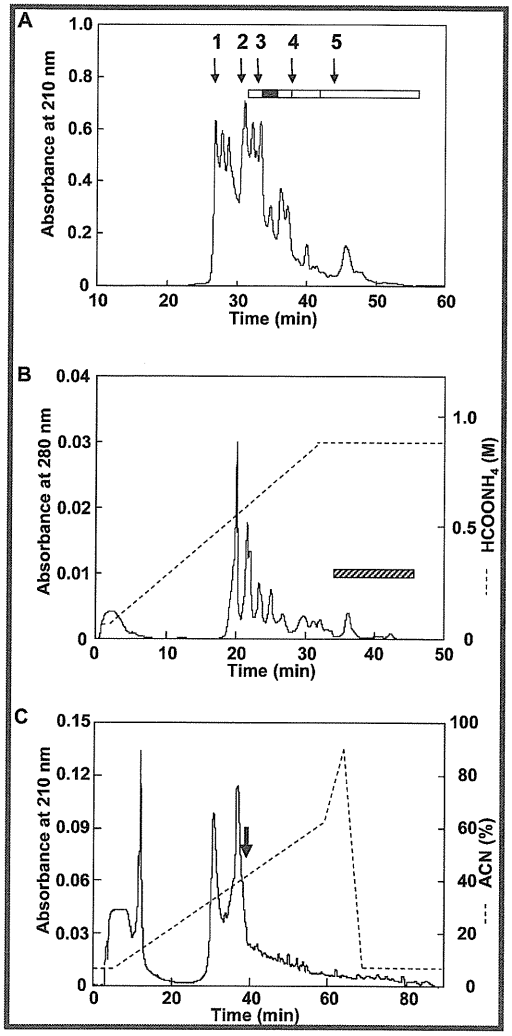


**Figure 1.** Preparation of highly basic peptides for peptidomic analysis. (A) Gel filtration profile of culture supernatant extracts from QGP-1 cells. Peptide-containing fractions were indicated by five boxes; the closed box indicated the fraction in which AMP-IBP5 originated. Molecular weight makers: 1, bovine serum albumin (66.5 kDa); 2, ribonuclease A (13.5 kDa); 3, neuropeptide Y (4.3 kDa); 4, neurotensin (1.7 kDa) and 5, Leu-enkephalin (0.6 kDa). (B) Cation-exchange HPLC of the AMP-IBP5-containing fraction obtained by the preceding gel filtration. Fractions eluted between 35 and 46 min (hatched box) were pooled for LC-MALDI-MS. (C) Subsequent nanoLC separation of the fraction denoted by the hatched box in (B). AMP-IBP5 was identified at the arrowed microfraction.

Signaling Technology). Membranes were visualized using an ECL-plus kit, according to the protocol provided by the manufacturer (GE Healthcare), and images were recorded with a LAS-1000 plus imager (Fujifilm, Tokyo, Japan) for 1−10 min. Digital images were quantitated using Image J software (National Institutes of Health, Bethesda, MD).

## RESULTS

### Peptidomic Identification of IGFBP-5-Derived Peptides

We recovered the culture supernatant from QGP-1 cells that received an exocytotic stimulus of 10 $\mu$M forskolin plus 10 $\mu$M carbachol for 15 min. Substances extracted from the supernatant were separated by gel filtration HPLC to obtain peptides

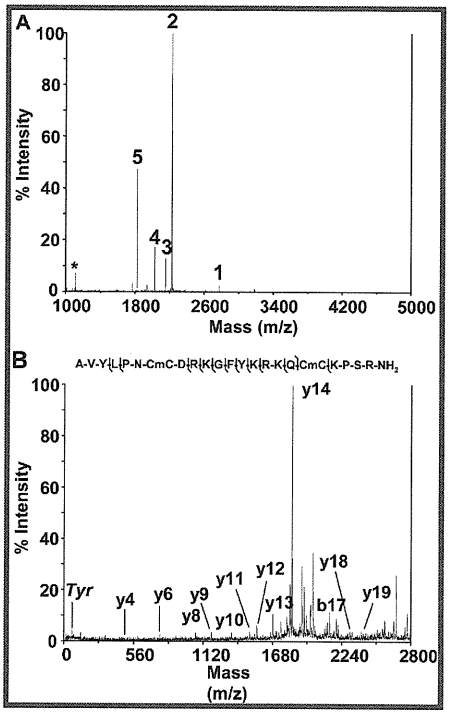


**Figure 2.** MS identification of AMP-IBP5. (A) MS spectrum from the microfraction indicated by the arrow in Figure 1C. 1, IGFBP-5[193-214]-$NH_2$ (AMP-IBP5) AVYLPNCDRKGFYKRKQCKPSR-$NH_2$; 2, VGF[543-561] HYHHALPPSRHYPGREAQA; 3, VGF[543-560]; 4, VGF[543-559]; 5, Desmoglein 2[10-24] NENKLLPKHPHLVRQ; *, double charged ions of 2. (B) MS/MS identification of AMP-IBP5. The peptide was identified with one b-ion and eleven y-ions. *Tyr* denotes the immonium ion of Tyr.

distributed over five fractions (Figure 1A, open and closed boxes). These five fractions were each subjected to reductive alkylation and further separated by cation-exchange HPLC (Figure 1B). To obtain a highly basic fraction, peptides eluted over the ammonium formate concentration of 0.9 M (pH 3.8) (Figure 1B, hatched box) were pooled for subsequent LC-MALDI-MS analysis. Table 1 summarizes a list of MS/MS-identified peptides in these basic fractions obtained by the cation-exchange separations. We identified 37 peptides, of which 35 peptides arose from precursor proteins reported to be enriched in secretory granules,[4,18] including VGF, somatostatin, prohormone convertase 2 (PC2), chromogranin A, chromogranin B, calcitonin gene-related peptide, calcitonin and nucleobindin 1. Among the identified peptides, AVYLPN(CmC)DRKGFYKRKQ(CmC)KPSR-$NH_2$ was derived from IGFBP-5 and found to be unique with a net charge of +7 even at pH 7.0 (Table 1). The closed box (Figure 1A), the hatched box (Figure 1B) and the arrow (Figure 1C) indicate the fractions in which this peptide originated. MS profiling of the microfraction indicated by the arrow in Figure 1C showed the signal of this peptide (Figure 2A, peak 1), whose sequence was identified by MS/MS (Figure 2B and Supplementary data).

IGFBP-5 is a secreted protein, but its proteolytic processing and concomitant generation of functional peptides remained unknown. To search for different IGFBP-5-derived peptides, we analyzed other fractions of the secretopeptidome by LC-MALDI-MS/MS. As shown in Table 2 and Figure 3, we identified a total of eight distinct peptides derived from IGFBP-5. This result

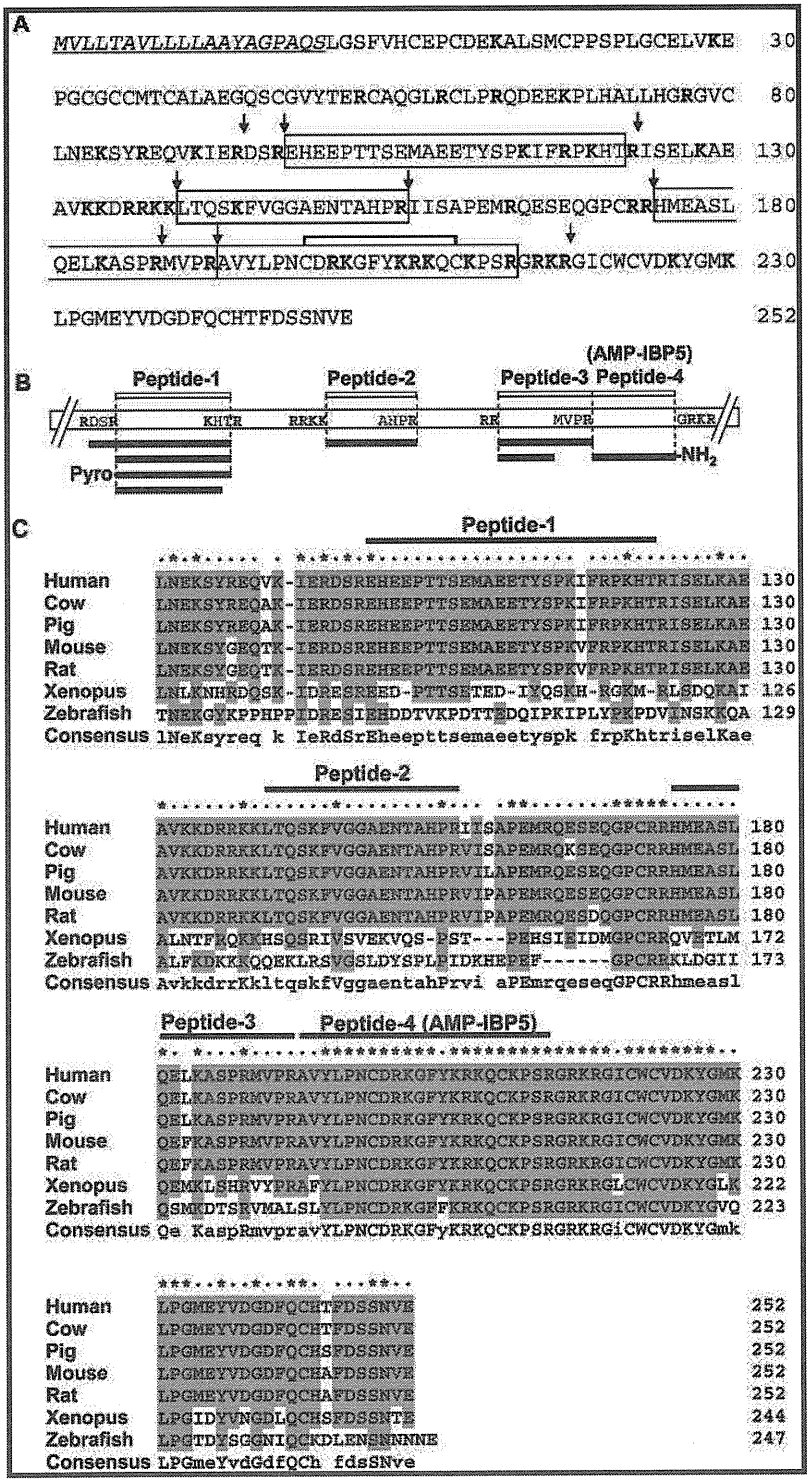


**Figure 3.** Peptides processed from IGFBP-5 and sequence alignment of IGFBP-5 between various vertebrates. (A) Amino acid sequence of human IGFBP-5. Signal sequence is indicated in italic and underlined. Basic amino acids, K and R, are denoted by bold letters. Four distinct regions from which peptides are processed out are boxed as follows: Peptide-1, IGFBP-5[98-122]; Peptide-2, IGFBP-5[140-156]; Peptide-3, IGFBP-5[175-192]; Peptide-4 (AMP-IBP5), IGFBP-5[193-214]-$NH_2$. The disulfide-bond (C199-C210) determined in this study is shown by the bold line. Processing sites predicted by identified peptides (Figure 3B) are indicated by arrows. (B) Identified peptides derived from IGFBP-5. Peptides listed in Table 2 are denoted by closed boxes. Above the entire precursor, open boxes indicate synthesized peptides. Basic amino acids in the processing sites are denoted by bold letters. Pyro- and -$NH_2$ mean N-terminal pyroglutamination and C-terminal amidation, respectively. (C) Sequence alignment of the central and C-terminal domains of various vertebrate IGFBP-5s. Residues conserved in more than four species are shaded. Asterisks indicate the completely conserved residues and dots indicate residues conserved in more than four vertebrates. Consensus amino acid residues conserved completely and in more than four species are indicated by upper and lower cases, respectively. Accession numbers of IGFBP-5: human, NP_000590.1; cow, NP_001098797.1; pig, NP_999264.1; mouse, NP_034648.2; rat, NP_036949.1; *Xenopus*, NP_001083938.1; and zebrafish, NP_991289.1. Residue numbering for zebrafish is based on the signal sequence prediction by SignalIP 3.0 Server (http://www.cbs.dtu.dk/services/SignalP/).

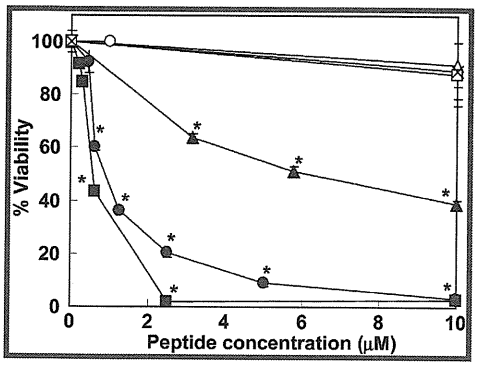


**Figure 4.** Antimicrobial activity of AMP-IBP5 against *Escherichia coli* K12. Increasing amounts of AMP-IBP5 (●, 0.3 to 10 μM) were mixed with *E. coli* K12 and incubated for 1 h at 37 °C. Antimicrobial activity was assayed as described under "Experimental procedures." Other IGFBP-5-derived peptides, Peptide-1 (Δ, 10 μM), Peptide-2 (□, 10 μM) and Peptide-3 (×, 10 μM), and IGFBP-5 protein (○, 1 μM) were also mixed with *E. coli* K12 and incubated as described above. As a positive control, increasing amounts of β-defensin-2 (▲, 3.2 to 10 μM) and cathelicidin (■, 0.2 to 10 μM) were used.

suggests that IGFBP-5 undergoes proteolytic processing to produce some functional peptides.

In neurons and endocrine cells, many peptides released by exocytosis are processed by PC1/3 or PC2.[19,20] Identification of the PC2-derived peptides, corresponding to the propeptide region, suggests the expression of functional PC2 in the cell line examined (Table 1). We deduced processing sites of the eight peptides from IGFBP-5 while considering their sequence information (Figure 3A) as well as substrate specificity of the PCs.[19,20] **RDSR**, **KHTR**, **RRKK**, **RR**, and **GRKR** shown in Figure 3B are typical processing sites for the PCs. We surmised that peptides are processed out from four distinct regions of this precursor protein, tentatively designated Peptide-1 to Peptide-4 in the order from N-terminus, and synthesized these peptides (Figure 3A). At the amino acid sequence level, Peptide-4 is completely identical among mammals and highly homologous between mammals and nonmammals (*Xenopus* and zebrafish) (Figure 3C). Collectively, this high sequence conservation of Peptide-4 suggests that this peptide contains a biologically active unit. Moreover, a consensus sequence for heparin binding XBBBXXBX (where X is a hydrophobic or uncharged residue and B is a basic residue)[10] is present in Peptide-4 (13YKRKQCKP20). In contrast with Peptide-4, Peptide-1 to Peptide-3 did not show marked homology between mammals and nonmammals (Figure 3C).

### Antimicrobial Activity of IGFBP-5-Derived Peptides

Cationic peptides that contain heparin-binding consensus sequences have been shown to exert antimicrobial activity.[10] Peptide-4 as well as cathelicidin bound to heparin, while Peptide-1 to Peptide-3 did not (Supplementary Figure 1C, F, Supporting Information). These results, in addition to the extremely basic nature of Peptide-4 with a net charge of +7 at pH 7.0 (Table 1), suggested that Peptide-4 exerts antimicrobial activity which we examined using a metabolic indicator alamarBlue™. Peptide-4 showed a significant antimicrobial activity against *E. coli* K12 at more than 0.6 μM, while Peptide-1 to Peptide-3 were not effective against *E. coli* K12 even at 10 μM (Figure 4). The $IC_{50}$ value of Peptide-4 was almost equal to or lower than those for well-characterized AMPs cathelicidin and β-defensin-2. These values for the known AMPs are consistent with those reported in previous studies.[21,22] Notably, the parent protein IGFBP-5 was ineffective even at 1 μM (Figure 4). Given these data, we renamed Peptide-4 as AMP-IBP5 (antimicrobial peptide derived from IGFBP-5).

To determine the antimicrobial spectrum of AMP-IBP5, we tested four-types of Gram-positive bacteria (*E. hirae*, *M. luteus*, *S. aureus* 209P and *S. saprophyticus* KD), two other Gram-negative bacteria (*E. coli* B and *E. coli* kp) and one fungus (*P. pastoris* GS115) (Table 3). AMP-IBP5 showed a broad and strong spectrum of antimicrobial activity except for two types of Gram-positive bacteria (*E. hirae* and *S. saprophyticus* KD). Of note, AMP-IBP5 was active against *M. luteus* and *P. pastoris* GS115, even greater than cathelicidin and β-defensin-2. AMP-IBP5 showed the activity against *S. aureus* 209P, *E. coli* B and *E. coli* kp, which were weaker than cathelicidin and greater than β-defensin-2. These results indicate that AMP-IBP5 shows an antimicrobial spectrum and activity almost equal to cathelicidin and greater than β-defensin-2.

We next assessed CAM-AMP-IBP5 to investigate the role of a disulfide linkage. Cysteine-rich AMPs such as defensins are structurally stabilized by intramolecular disulfide linkages that are essential for their function.[23] In fact, CAM-β-defensin-2 did not show antimicrobial activity against various bacteria except for *M. luteus*, to which it was still active, though more than five-fold weaker than the intact form (Table 3). As for CAM-AMP-IBP5, antimicrobial activity was abrogated for *S. aureus* 209P and *E. coli* kp. On the other hand, this peptide retained the activity against *M. luteus*, *E. coli* B and *P. pastoris* GS115 comparable to the intact peptide, while the modified peptide showed about 2-fold weaker activity against *E. coli* K12 than the intact peptide. These results indicate that the disruption of disulfide linkages in AMP-IBP5 is less effective in reducing antimicrobial activity than that in β-defensin-2 presumably because the former contains only one disulfide linkage while the latter contains three disulfide linkages.

Some AMPs have the C-terminal amide group that plays a significant role in their antimicrobial properties.[24,25] We measured antimicrobial activity of C-terminally Gly-extended AMP-IBP5 to evaluate the contribution of the C-terminal amide group. It showed no activity against *S. aureus* 209P, *E. coli* B and *E. coli* kp as well as *E. hirae* and *S. saprophyticus* KD. On the other hand, this peptide retained the activity against *M. luteus* and *P. pastoris* GS115 comparable to the intact peptide, while the modified peptide was about 10-fold weaker against *E. coli* K12 than the intact peptide. These results indicate that the C-terminal amide group of AMP-IBP5 is important for its activity.

To examine whether AMP-IBP5 is bactericidal or just bacteriostatic, we performed a classical colony formation assay. It has been established that the bactericidal peptide concentration revealed by classical colony formation assays and the alamarBlue™ assay shows a good agreement.[26−28] As expected, this peptide showed strong antimicrobial activity with $IC_{50}$ of 1.6, 1.1, and 0.4 μM against *S. aureus* 209P, *E. coli* K12 and *P. pastoris* GS115, respectively (Table 4). These $IC_{50}$ values were also almost equal to or lower than that for cathelicidin and β-defensin-2 as in the case of the alamarBlue assay. These results indicate that AMP-IBP5 is bactericidal against these bacteria.

### Immunological and Mass Spectrometric Characterization of IR-AMP-IBP5

We developed a RIA system specific to the C-terminal region including amide structure (see "Experimental Procedures") to

**Table 3. Antimicrobial Activity of AMP-IBP5, β-Defensin-2, and Cathelicidin (alamarBlue Assay)**

| | $IC_{50}(\mu M)$[a] | | | | | |
|---|---|---|---|---|---|---|
| | AMP-IBP5 | | | β-defensin-2 | | cathelicidin |
| Bacteria | intact[b] | CAM[b] | C-Gly[b] | intact[b] | CAM[b] | intact[b] |
| Gram-positive bacteria | | | | | | |
| *Enterococcus hirae* | >10 | >10 | >10 | 2.4 | >10 | 0.3 |
| *Micrococcus luteus* | 0.5 | 0.7 | 0.8 | 0.7 | 3.9 | 1.3 |
| *Staphylococcus aureus* 209 P | 0.8 | >10 | >10 | 8.6 | >10 | 0.3 |
| *Staphylococcus saprophyticus* KD | >10 | >10 | >10 | >10 | >10 | 0.6 |
| Gram-negative bacteria | | | | | | |
| *Escherichia coli* B | 8.8 | 7.6 | >10 | >10 | >10 | 0.5 |
| *Escherichia coli* K12 | 0.9 | 2.2 | 9.3 | 6.3 | >10 | 0.6 |
| *Escherichia coli* kp | 4.2 | >10 | >10 | 7.4 | >10 | 1.7 |
| Fungi | | | | | | |
| *Pichia pastoris* GS115 | 1.3 | 1.5 | 1.6 | 2.6 | >10 | 3.1 |

[a] Fifty percent growth inhibitory concentration. [b] Intact, intact peptide; CAM, carbamidomethylated peptide; C-Gly, C-terminally Gly-extended peptide.

**Table 4. Antimicrobial Activity of AMP-IBP5, β-Defensin-2, and Cathelicidin (Colony Formation Assay)**

| | $IC_{50}$ ($\mu M$) | | |
|---|---|---|---|
| | AMP-IBP5 | β-defensin-2 | cathelicidin |
| Gram-positive bacteria | | | |
| *Staphylococcus aureus* 209 P | 1.6 | 3.9 | 0.03 |
| Gram-negative bacteria | | | |
| *Escherichia coli* K12 | 1.1 | >10 | 0.4 |
| Fungi | | | |
| *Pichia pastoris* GS115 | 0.4 | 1.0 | 1.2 |

determine IR-AMP-IBP5 levels released from QGP-1 cells with or without stimulation by carbachol plus forskolin (10 $\mu$M each) for 15 min. The exocytosis stimulus caused a 500-fold increase in IR-AMP-IBP5 levels; the amounts secreted per $10^7$ cells before and after 15-min stimulation were 4.9 fmol and 2.6 pmol, respectively. We also determined IR-AMP-IBP5 levels released from SHP-77 cells with or without stimulation by carbachol (10 $\mu$M) plus potassium chloride (50 mM) for 10 min. The exocytosis stimulus caused a 5-fold increase in IR-AMP-IBP5 levels; the amounts secreted per $10^7$ cells before and after 10-min stimulation were 140 fmol and 650 fmol, respectively.

We determined AMP-IBP5 levels in rat tissues using the same RIA system. IR-AMP-IBP5 in the brain, pituitary gland and small intestine was 2.1, 6.2, and 1.5 pmol/g wet tissues, respectively. In the lung, heart, stomach, liver, pancreas, kidney and uterus, it was below the detection limit for quantitative measurement (0.6 pmol/g wet tissue) (Figure 5). On the other hand, intact IGFBP-5 protein was detected in the brain, pituitary gland, heart, stomach and kidney, while GAPDH was detected in all tissues tested by Western blot analysis (Supplementary Figure 2, Supporting Information). Judging from these results, the extent of IGFBP-5 processing to AMP-IBP5 was different in each tissue.

IR-AMP-IBP5 in rat brain extract was characterized by chromatographies. In gel filtration on a Sephadex G-50 column, IR-AMP-IBP5 occurred as a distinctive peak in the region of relative

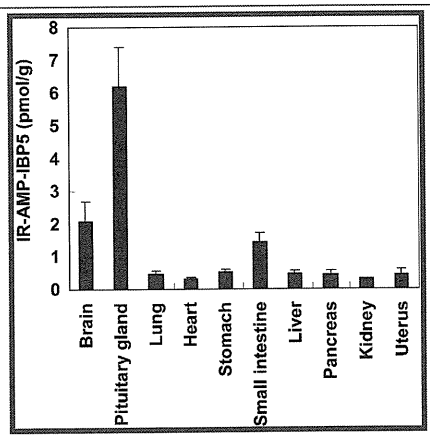


**Figure 5.** Determination of IR-AMP-IBP5 levels in rat tissues by RIA. Data are the mean ± SD ($n$ = 3). The detection limit for quantitative measurement is 0.6 pmol/g wet tissues.

molecular mass less than 4 kDa (Figure 6A). Subsequently, we separated the IR-AMP-IBP5-rich fractions (Figure 6A, open box) using reverse phase HPLC and obtained two major peaks of IR-AMP-IBP5 (Figure 6B). The peak eluted earlier (Figure 6B, open arrow) behaved consistently with synthetic AMP-IBP5, while the peak eluted later remained unidentified. To identify the major endogenous molecular form, we analyzed the earlier eluted peak by MS of immunoprecipitates, and obtained a dominant peak at $m/z$ 2654.3 ($[M + H]^+$ ion) (Figure 6C). This mass value corresponded to the theoretical mass of synthetic AMP-IBP5 ($m/z$, 2654.4), which was calculated as a disulfide-linked, C-terminally amidated peptide from rat IGFBP-5[193-214].

We characterized IR-AMP-IBP5 also in small intestine extract. As in the brain, most immunoreactivity was observed less than 4 kDa in the gel filtration chromatography (Supplementary Figure 3A, Supporting Information) and separated into two major peaks of IR-AMP-IBP5 by reverse phase HPLC (Supplementary Figure 3B). The earlier eluted peak (Supplementary Figure 3B, open arrow, Supporting Information) was consistent with synthetic AMP-IBP5, as assessed by the retention time. MS

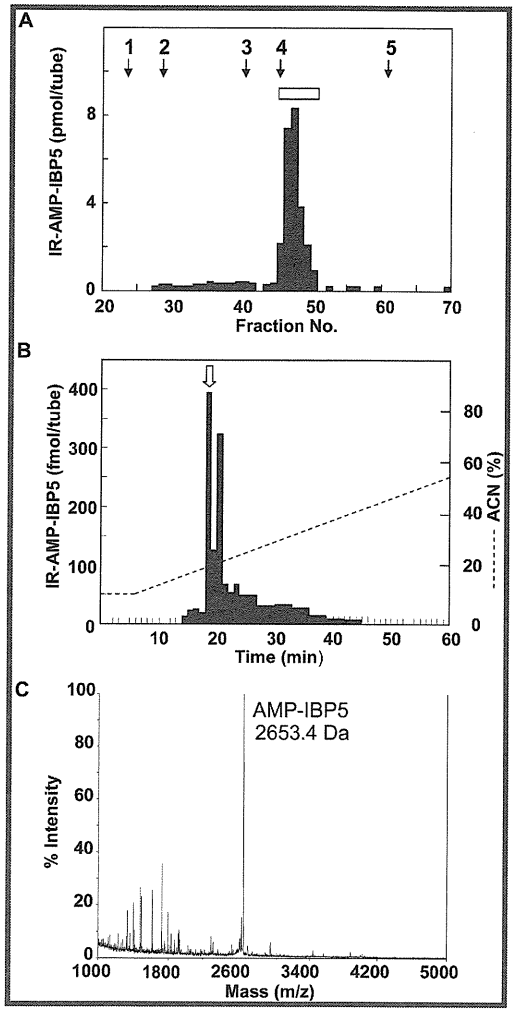


**Figure 6.** Characterization and identification of IR-AMP-IBP5 in rat brain extract. (A) Gel filtration of a brain extract (15-g equivalents). Molecular weight makers: 1, $V_0$; 2, bovine serum albumin (66.5 kDa); 3, ribonuclease A (13.5 kDa); 4, neuropeptide Y (4.3 kDa); 5, $V_t$. Fractions 46−50 (open box) were pooled for reverse phase HPLC. (B) Subsequent reverse phase HPLC of 1/8 amounts of the fractions obtained by the gel filtration. Synthetic AMP-IBP5 was eluted at the arrowed position. (C) MS analysis of peptides immunoprecipitated from the fraction indicated by the arrow in (B) with anti-AMP-IBP5 antiserum.

analysis of immunoprecipitates of the earlier eluted peak in Supplementary Figure 3B revealed a distinctive peak at $m/z$ 2654.4 ($[M + H]^+$ ion) (Supplementary Figure 3C, Supporting Information), consistent with the mass of synthetic AMP-IBP5.

## DISCUSSION

AMP-IBP5, as its name implies, is a novel AMP that arises from IGFBP-5 through specific processing. This peptide had a broad and strong spectrum of antimicrobial activity against bacteria and fungi. It should be noted, however, that the parent protein IGFBP-5 had no such activity. IGFBP-5 is increasingly recognized to have cellular functions independent of the insulin-like growth factor (IGF) receptor, as well as those dependent on the receptor.[29] To the best of our knowledge, this is the first report that IGFBP-5 produces a functional bioactive peptide.

To exert their antimicrobial effect, AMPs adhere to negatively charged membranes of pathogens, followed by displacement of lipids and alteration of the membrane structure.[30] In terms of antimicrobial spectrum and potency, AMP-IBP5 is comparable to well-characterized AMPs cathelicidin and $\beta$-defensin-2; AMP-IBP5 was effective against six microorganisms including *E. coli* K12 in the eight organisms tested. The C-terminally Gly-extended AMP-IBP5 reduced its antimicrobial activity compared to the native form (Table 3), as in other C-terminally amidated AMPs.[24,25] This finding suggests that AMP-IBP5 interacts electrostatically at its positive-charged region in the amphipathic structure with the negatively charged bacterial membranes.

QGP-1 cells express functional peptidyl-glycine alpha-amidating monooxygenase (PAM) localized in secretory granules.[31] They also express functional secretory granule marker enzymes PC1/3 and PC2, as evidenced by the identification of peptides corresponding to the propeptide region of each enzyme (unpublished data and Table 1). Most of the cleavage sites of the identified IGFBP-5-derived peptides agreed with the consensus sites recognized by PC1/3 or PC2 (Table 2 and Figure 3). Furthermore, upon stimulation, IR-AMP-IBP5 in culture medium of QGP-1 cells and SHP-77 cells was increased by 500-fold and 5-fold, respectively. These results suggest that AMP-IBP5 is stored in secretory granules and awaits secretion in response to exocytotic stimuli.

Consistent with its identification as a C-terminally amidated peptide, AMP-IBP5 flanks the amidation motif 215GRKR218 (Figure 3A). Since this stretch of basic residues agrees with a consensus recognition site for PC1/3 or PC2,[19,20] it is presumed that the site 218R↓G219 is first endoproteolytically cleaved by PC1/3 or PC2, followed by carboxypeptidase E-mediated removal of 216RKR218. As in many bioactive peptides, the upstream glycine G215 contributed to the PAM-mediated generation of the arginine amide structure.[20] The N-terminal flanking sequence, 189MVPR↓A193, is atypical for PC1/3 or PC2 cleavage. However, an example of cleavage C-terminal to a single arginine is seen in the N-terminus of neuromedin C, MYPR↓G,[32] which has recently been shown to be created by PC2.[33] Since the cleavage sites of AMP-IBP5 and neuromedin C are quite similar, PC2 may participate in AMP-IBP5 processing. These findings strongly suggest that AMP-IBP5 is generated by specific processing proteases.

IGFBP-5 belongs to the IGFBP family that consists of six well characterized members, IGFBP-1 to IGFBP-6. IGFBP-5 is known to consist of three domains;[8] N-terminal domain (residues 1-80), central domain (residues 81-170), and C-terminal domain (residues 171-252). One of the most notable sequence features common to IGFBPs is the presence of a large number of cysteine residues, the location of which is highly conserved among them. IGFBP-5 has 12 and 6 cysteine residues in the N- and C-terminal domains, respectively (Figure 3A). The IGF-binding domain in the N-terminal domain represents a rigid globular structure having in its core three antiparallel $\beta$-strands and two disulfide linkages (C47-C60 and C54-C80).[34] This rigid structure may be resistant to proteolysis or processing, and may explain why we failed to identify peptide fragments from the N-terminal domain (Table 2 and Figure 3B).

In general, identification of cysteine-containing peptides by MS/MS requires reductive alkylation of their cysteine residues. This conversion abolishes the physiological disulfide linkages of a target peptide. To determine a molecular mass of intact AMP-IBP5, we conducted immunoprecipitation experiments in a physiological nonreducing condition using antibody specific to the C-terminal structure. We observed a major peptide having a

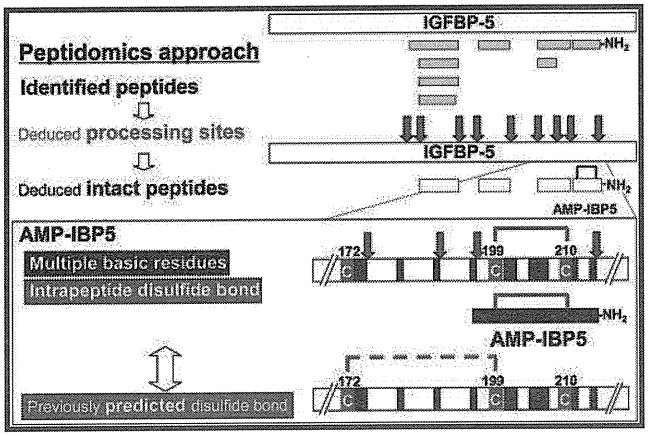


**Figure 7.** Peptidomics is indispensable for bioactive peptide discovery. Peptides released by exocytosis (gray boxes) were identified and utilized to predict processing sites (gray arrows) and resultant peptides (open boxes). Among the identified peptides was AMP-IBP-5 having two cysteine residues. The region surrounding AMP-IBP5 is close-up and boxed. The two cysteines (C199 and C210) forms a disulfide bond, which is confirmed by immunoprecipitation/MS conducted under nonreducing conditions. This disulfide bond argues against previous prediction (C172-C199, gray dashed line), which is inferred on the basis of analogy to IGFBP-4 and -6. In addition, AMP-IBP5 possesses multiple basic residues (closed boxes). Because of these structural properties, this peptide escapes identification by conventional proteomics or bioinformatics.

molecular mass of 2653.4 Da, consistent with the presence of an intramolecular disulfide linkage (C199-C210) in the condition that cysteine residues were left intact (Figure 6C and Supplementary Figure 3C, Supporting Information) along with C-terminal amidation. By analogy to IGFBP-4 and IGFBP-6, it has been previously inferred that C172-C199, C210-C221, and C223-C243 were disulfide-linked in the IGFBP-5 sequence[8] (Figure 7). However, we argue against this prediction and concluded that the pairing C199-C210 is physiologically relevant. Taken together, these findings strongly indicate that the IGFBP-5 disulfide linkage pattern is different from those of IGFBP-4 and IGFBP-6. It should be noted that bioinformatics approaches would not uncover this peptide so long as they rely on incorrect assumption about disulfide pairings.

## CONCLUSION

Using peptidomics techniques, we discovered a potent AMP derived from IGFBP-5, which is designated AMP-IBP5. We demonstrated that our peptidomic approach to predicting intact peptides and related processing sites through MS-identified peptide sequences has an advantage over bioinformatics-dependent prediction, especially for intramolecular disulfide-linked peptides such as AMP-IBP5. The generation of this peptide cannot be predicted by bioinformatics since disulfide bond patterns of IGFPB-5 are incorrectly inferred from related family members. In addition, the inability of conventional proteomics to identify peptides having internal multiple basic residues highlights the impact of peptidomics targeting naturally occurring peptides (Figure 7).

## ASSOCIATED CONTENT

### Supporting Information

Supplemental Figure 1, Heparin-binding analysis of IGFBP-5-derived peptides by reverse phase HPLC. Supplemental Figure 2, Evaluation of intact IGFBP-5 protein levels in rat tissues by Western blot analysis. Supplemental Figure 3, Characterization and identification of IR-AMP-IBP5 in rat small intestine. Supplemental data, MS/MS spectra of the peptides with modified residues listed in Tables 1 and 2, and those used for single peptide-based identification were also included. This material is available free of charge via the Internet at http://pubs.acs.org.

## AUTHOR INFORMATION

### Corresponding Author

*Department of Molecular Pharmacology, National Cerebral and Cardiovascular Center Research Institute, 5-7-1 Fujishirodai, Suita, Osaka 565-8565, Japan. Phone: +81-6-6833-5012 ext.2507. Fax: +81-6-6835-5349. E-mail: ksasaki@ri.ncvc.go.jp or minamino@ri.ncvc.go.jp.

## ACKNOWLEDGMENT

We are grateful to Prof. S. Kawabata of Kyushu University for helpful discussion and donation of bacteria; *E. hirae, M. luteus, S. aureus* 209P, *S. saprophyticus* KD, *E. coli* B, *E. coli* K12, *E. coli* kp and *P. pastoris* GS115. We also thank Ms. M. Nakatani for technical assistance. This work was supported in part by Grant-in-Aid for Young Scientists (B) (21770156) from the Japan Society for the Promotion of Science, by the Program for Promotion of Fundamental Studies in Health Sciences of the National Institute of Biomedical Innovation, and by the Intramural Research Fund of National Cerebral and Cardiovascular Center of Japan.

## ABBREVIATIONS

ACN, acetonitrile; AMP, antimicrobial peptide; AMP-IBP5, antimicrobial peptide derived from insulin-like growth factor-binding protein 5; CAM, carbamidomethylated; CmC, carbamidomethyl cysteine; *E. coli, Escherichia coli*; *E. hirae, Enterococcus hirae*; GAPDH, glyceraldehyde 3-phosphate dehydrogenase; HPLC, high performance liquid chromatography; $IC_{50}$, 50% inhibitory concentration; IGF, insulin-like growth factor; IGFBP-5, insulin-like growth factor-binding protein 5; IR, immunoreactive; LC, liquid chromatography; MALDI, matrix-assisted laser desorption/ionization; *M. luteus, Micrococcus luteus*; MS, mass spectrometry; MS/MS, tandem mass spectrometry; PAM, peptidyl-glycine alpha-amidating monooxygenase; PAMP-20, proadrenomedullin N-terminal 20-amino acid peptide; PBS, phosphate-buffered saline; PC2, prohormone convertase 2; *P. pastoris, Pichia pastoris*; RIA, radioimmunoassay; *S. aureus, Staphylococcus aureus*; SD, standard deviation; TFA, trifluoroacetic acid.

## REFERENCES

(1) Clynen, E.; Baggerman, G.; Veelaert, D.; Cerstiaens, A.; Van der Horst, D.; Harthoorn, L.; Derua, R.; Waelkens, E.; De Loof, A.; Schoofs, L. Peptidomics of the pars intercerebralis-corpus cardiacum complex of the migratory locust, *Locusta migratoria*. *Eur. J. Biochem.* **2001**, *268*, 1929–1939.

(2) Schrader, M.; Schulz-Knappe, P. Peptidomics technologies for human body fluids. *Trends Biotechnol.* **2001**, *19*, S55–60.

(3) Boonen, K.; Baggerman, G.; D'Hertog, W.; Husson, S. J.; Overbergh, L.; Mathieu, C.; Schoofs, L. Neuropeptides of the islets of Langerhans: a peptidomics study. *Gen. Comp. Endocrinol.* **2007**, *152*, 231–241.

(4) Sasaki, K.; Satomi, Y.; Takao, T.; Minamino, N. Snapshot peptidomics of the regulated secretory pathway. *Mol. Cell. Proteomics* **2009**, *8*, 1638–1647.

(5) Sasaki, K.; Takahashi, N.; Satoh, M.; Yamasaki, M.; Minamino, N. A peptidomics strategy for discovering endogenous bioactive peptides. *J. Proteome Res.* **2010**, *9*, 5047–5052.

(6) Harder, J.; Bartels, J.; Christophers, E.; Schröder, J. M. A peptide antibiotic from human skin. *Nature* **1997**, *387*, 861.

(7) Gudmundsson, G. H.; Agerberth, B.; Odeberg, J.; Bergman, T.; Olsson, B.; Salcedo, R. The human gene FALL39 and processing of the cathelin precursor to the antibacterial peptide LL-37 in granulocytes. *Eur. J. Biochem.* **1996**, *238*, 325–332.

(8) Beattie, J.; Allan, G. J.; Lochrie, J. D.; Flint, D. J. Insulin-like growth factor-binding protein-5 (IGFBP-5): a critical member of the IGF axis. *Biochem. J.* **2006**, *395*, 1–19.

(9) Kaku, M.; Nishiyama, T.; Yagawa, K.; Abe, M. Establishment of a carcinoembryonic antigen-producing cell line from human pancreatic carcinoma. *Gann* **1980**, *71*, 596–601.

(10) Andersson, E.; Rydengård, V.; Sonesson, A.; Mörgelin, M.; Björck, L.; Schmidtchen, A. Antimicrobial activities of heparin-binding peptides. *Eur. J. Biochem.* **2004**, *271*, 1219–1226.

(11) Saito, T.; Kawabata, S.; Sigenaga, T.; Takayenoki, Y.; Cho, J.; Nakajima, H.; Hirata, M.; Iwanaga, S. A novel big defensin identified in horseshoe crab hemocytes: isolation, amino acid sequence, and antibacterial activity. *J. Biochem.* **1995**, *117*, 1131–1137.

(12) Osaki, T.; Omotezako, M.; Nagayama, R.; Hirata, M.; Iwanaga, S.; Kasahara, J.; Hattori, J.; Ito, I.; Sugiyama, H.; Kawabata, S. Horseshoe crab hemocyte-derived antimicrobial polypeptides, tachystatins, with sequence similarity to spider neurotoxins. *J. Biol. Chem.* **1999**, *274*, 26172–26178.

(13) Fisher, E. R.; Paulson, J. D. A new in vitro cell line established from human large cell variant of oat cell lung cancer. *Cancer Res.* **1978**, *38*, 3830–38359.

(14) Katafuchi, T.; Kikumoto, K.; Hamano, K.; Kangawa, K.; Matsuo, H.; Minamino, N. Calcitonin receptor-stimulating peptide, a new member of the calcitonin gene-related peptide family. Its isolation from porcine brain, structure, tissue distribution, and biological activity. *J. Biol. Chem.* **2003**, *278*, 12046–12054.

(15) Yamaguchi, H.; Sasaki, K.; Satomi, Y.; Shimbara, T.; Kageyama, H.; Mondal, M. S.; Toshinai, K.; Date, Y.; González, L. J.; Shioda, S.; Takao, T.; Nakazato, M.; Minamino, N. Peptidomic identification and biological validation of neuroendocrine regulatory peptide-1 and -2. *J. Biol. Chem.* **2007**, *282*, 26354–26360.

(16) Shoji, H.; Minamino, N.; Kangawa, K.; Matsuo, H. Endotoxin markedly elevates plasma concentration and gene transcription of adrenomedullin in rat. *Biochem. Biophys. Res. Commun.* **1995**, *215*, 531–537.

(17) Osaki, T.; Okino, N.; Tokunaga, F.; Iwanaga, S.; Kawabata, S. Proline-rich cell surface antigens of horseshoe crab hemocytes are substrates for protein cross-linking with a clotting protein coagulin. *J. Biol. Chem.* **2002**, *277*, 40084–40090.

(18) Brunner, Y.; Coute, Y.; Lezzi, M.; Foti, M.; Fukuda, M.; Hochstrasser, D. F.; Wollheim, C. B.; Sanchez, J.-C. Proteomics analysis of insulin secretory granules. *Mol. Cell. Proteomics* **2007**, *6*, 1007–1017.

(19) Zhou, A.; Webb, G.; Zhu, X.; Steiner, D. F. Proteolytic processing in the secretory pathway. *J. Biol. Chem.* **1999**, *274*, 20745–20748.

(20) Fricker, L. D. Neuropeptide-processing enzymes: applications for drug discovery. *AAPS J.* **2005**, *7*, E449–455.

(21) Travis, S. M.; Anderson, N. N.; Forsyth, W. R.; Espiritu, C.; Conway, B. D.; Greenberg, E. P.; McCray, P. B., Jr; Lehrer, R. I.; Welsh, M. J.; Tack, B. F. Bactericidal activity of mammalian cathelicidin-derived peptides. *Infect. Immun.* **2000**, *68*, 2748–2755.

(22) Bals, R.; Wang, X.; Wu, Z.; Freeman, T.; Bafna, V.; Zasloff, M.; Wilson, J. M. Human beta-defensin 2 is a salt-sensitive peptide antibiotic expressed in human lung. *J. Clin. Invest.* **1998**, *102*, 874–880.

(23) Bauer, F.; Schweimer, K.; Klüver, E.; Conejo-Garcia, J. R.; Forssmann, W. G.; Rösch, P.; Adermann, K.; Sticht, H. Structure determination of human and murine beta-defensins reveals structural conservation in the absence of significant sequence similarity. *Protein Sci.* **2001**, *10*, 2470–2479.

(24) Suetake, T.; Aizawa, T.; Koganesawa, N.; Osaki, T.; Kobashigawa, Y.; Demura, M.; Kawabata, S.; Kawano, K.; Tsuda, S.; Nitta, K. Production and characterization of recombinant tachycitin, the Cys-rich chitin-binding protein. *Protein Eng.* **2002**, *15*, 763–769.

(25) Dos Santos Cabrera, M. P.; Arcisio-Miranda, M.; Broggio Costa, S. T.; Konno, K.; Ruggiero, J. R.; Procopio, J.; Ruggiero Neto, J. Study of the mechanism of action of anoplin, a helical antimicrobial decapeptide with ion channel-like activity, and the role of the amidated C-terminus. *J. Pept. Sci.* **2008**, *14*, 661–669.

(26) Tenover, F.; Swenson, J. M.; O'Hara, C. M.; Stocker, S. A. Ability of commercial and reference antimicrobial and reference antimicrobial susceptibility testing methods to detect vancomycin resistance in enterococci. *J. Clin. Microbiol.* **1995**, *33*, 1524–1527.

(27) Yajko, D. M.; Madej, J. J.; Lancaster, M. V.; Sanders, C. A.; Cawthon, V. L.; Gee, B.; Babst, A.; Hadley, W. K. Colorimetric method for determining MICs of antimicrobial agents for Mycrobacterium tuberculosis. *J. Clin. Microbiol.* **1995**, *33*, 2324–2327.

(28) DeForge, L. E.; Billeci, K. L.; Kramer, S. M. Effect of IFN-$\gamma$ on the killing of *S. aureus* in human whole blood. Assessment of bacterial viability by CFU determination and by a new method using alamarBlue. *J. Immunol. Methods* **2000**, *245*, 79–89.

(29) Firth, S. M.; Baxter, R. C. Cellular actions of the insulin-like growth factor binding proteins. *Endocr. Rev.* **2002**, *23*, 824–854.

(30) Zasloff, M. Antimicrobial peptides of multicellular organisms. *Nature* **2002**, *415*, 389–395.

(31) Tateishi, K.; Arakawa, F.; Misumi, Y.; Treston, A. M.; Vos, M.; Matsuoka, Y. Isolation and functional expression of human pancreatic peptidylglycine alpha-amidating monooxygenase. *Biochem. Biophys. Res. Commun.* **1994**, *205*, 282–290.

(32) Minamino, N.; Kangawa, K.; Matsuo, H. Neuromedin C: a bombesin-like peptide identified in porcine spinal cord. *Biochem. Biophys. Res. Commun.* **1984**, *119*, 14–20.

(33) Zhang, X.; Pan, H.; Peng, B.; Steiner, D. F.; Pintart, J. E.; Fricker, L. D. Neuropeptidomic analysis establishes a major role for prohormone convertase-2 in neuropeptide biosynthesis. *J. Neurochem.* **2010**, *112*, 1168–1179.

(34) Kalus, W.; Zweckstetter, M.; Renner, C.; Sanchez, Y.; Georgescu, J.; Grol, M.; Demuth, D.; Schumacher, R.; Dony, C.; Lang, K.; Holak, T. A. Structure of the IGF-binding domain of the insulin-like growth factor-binding protein-5 (IGFBP-5): implications for IGF and IGF-I receptor interactions. *EMBO J.* **1998**, *17*, 6558–6572.

Special

# Japanese-Western Consensus Meeting on Biomarkers

## Executive Summary

Alan S. MAISEL,[1] MD, Kazuwa NAKAO,[2] MD, Piotr PONIKOWSKI,[3] MD, W. Frank PEACOCK,[4] MD, Michihiro YOSHIMURA,[5] MD, Toru SUZUKI,[6] MD, Takayoshi TSUTAMOTO,[7] MD, Gerasimos S. FILIPPATOS,[8] MD, Yoshihiko SAITO,[9] MD, Yoshihiko SEINO,[10] MD, Naoto MINAMINO,[11] PhD, Yasunobu HIRATA,[6] MD, Masashi MUKOYAMA,[2] MD, Toshio NISHIKIMI,[2] MD, *and* Ryozo NAGAI,[6] MD

On November 21, 2009, biomarker leaders from Europe and America met with leading biomarker and cardiac leaders of Japan to discuss and come to consensus on state-of-the-art natriuretic peptide research. Natriuretic peptides, brain natriuretic peptide (BNP) and N-terminal pro-brain natriuretic peptide (NT-proBNP), have revolutionized the way we look at patients presenting with dyspnea. While not considered stand-alone tests, natriuretic peptide (NP) testing clearly adds value to the workup and follow-up of patients. In order to use NP levels correctly, physicians need to be aware of the molecular biology of the peptides, appropriate cutoffs in various conditions, and important caveats for using natriuretic peptide levels. These were all discussed at the meeting. Additionally, natriuretic peptide testing as portrayed in guidelines from the participating countries were compared and contrasted. When describing BNP values in Japan and in the United States in parallel, each BNP value was calculated by using the correlation data of Fischer *et al.*[1] (Int Heart J 2011; 52: 253-265)

**State-of-the-art BNP research:** Brain natriuretic peptide (BNP) first isolated from the porcine brain is a cardiac hormone secreted mainly from the ventricle of the heart. Human BNP consists of 32 amino acids, and its molecular size differs from those of other species. The primary structure of BNP also shows marked species difference as shown in Figure 1, indicating that the specificity of the antibody used for the assay system should be carefully considered. Metabolic clearance of natriuretic peptide family, atrial natriuretic peptide (ANP), BNP and C-type natriuretic peptide (CNP) comprises two systems, neutral endopeptidase-mediated degradation and clearance receptor-mediated internalization. The rank order in affinity for human clearance receptor is ANP > CNP > BNP, indicating that the half life of BNP in the bloodstream is longer than those of ANP and CNP. In striking contrast with molecular forms of ANP in plasma and the heart, the molecular forms of BNP consist of proBNP and BNP in humans as well as in rats. Table I shows a comparison of BNP and ANP in various aspects. Although a recent paper reported that BNP does not circulate in patients with heart failure, which indicates proBNP functions as a circulating form of BNP-like immunoreactivity in human plasma, this misleading result can be explained by the very poor recovery of BNP-32 extraction and peptidase digestion of BNP-32. The posttranslational processing of proBNP is more advanced in the central nervous system. The modification by O-glycosylation of the N-terminal part of proBNP, which interferes with the processing of proBNP, makes precise analysis of molecular forms of circulating BNP-like and N-terminal proBNP-like immunoreactivities very difficult for clinical biomarkers. Since the functional molecule of BNP is BNP-32, and BNP-32 is not modified by O-glycosylation and other modifications, BNP-32 should be measured as a biomarker for heart failure (HF), like insulin for diabetes mellitus as shown in Table II.

**Complex BNP species in human plasma:** BNP is a clinically useful diagnostic marker for pathophysiological conditions of heart disease, including HF, ventricular remodeling, and pulmonary hypertension.[2,3] BNP-32 (active form), proBNP (proBNP[1-108], weakly active form), and NT-proBNP (proBNP[1-76], inactive form) circulate in the plasma of healthy subjects in contrast with atrial natriuretic peptide (ANP) (Figure 2). Although plasma levels of these BNP species increase in HF patients, recent studies have revealed that the plasma proBNP level shows a higher elevation than that of BNP-32.[4,5] In the plasma of HF patients, furthermore, proBNP is O-glycosylated in the NT-proBNP region, and O-glycosylated (Glyco-) proBNP with weak activity circulates along with Glyco-NT-proBNP and other known BNP species (Figures 2 and 3).[6,7] Commercially available BNP assay kits, such as from Shionogi and Abbott, utilize antibodies directed against a ring or a C-terminal portion of BNP-32, which cross-react with proBNP to comparable or lesser extents.[8,9] Glyco-NT-proBNP is less reactive in NT-proBNP assay kits, such as from Roche, and is underestimated as indicated by recovery of its immunoreactiv-

From the [1] Division of Cardiology, Department of Medicine, University of California, California, United States of America, [2] Department of Medicine and Clinical Science, Kyoto University Graduate School of Medicine, Kyoto, Japan, [3] Department of Heart Diseases Medical University, Clinical Military Hospital, Wroclaw, Poland, [4] Department of Emergency Medicine, Cleveland Clinic, Ohio, United States of America, [5] Division of Cardiology, Department of Internal Medicine, The Jikei University School of Medicine, [6] Department of Cardiovascular Medicine, Graduate School of Medicine, The University of Tokyo, Tokyo, [7] Toyosato Hospital, Shiga, [8] University of Athens, Athens, Greece, [9] First Department of Internal Medicine, Nara Medical University, Nara, [10] Cardiovascular Center, Department of Cardiology, Nippon Medical School Chiba-Hokuso Hospital, Chiba, and [11] Department of Molecular Pharmacology, National Cerebral and Cardiovascular Center Research Institute, Osaka, Japan.

Address for correspondence: Alan S. Maisel, Division of Cardiology, Department of Medicine, University of California, San Diego, CA, USA.

Received for publication May 2, 2011.

Accepted May 2, 2011.

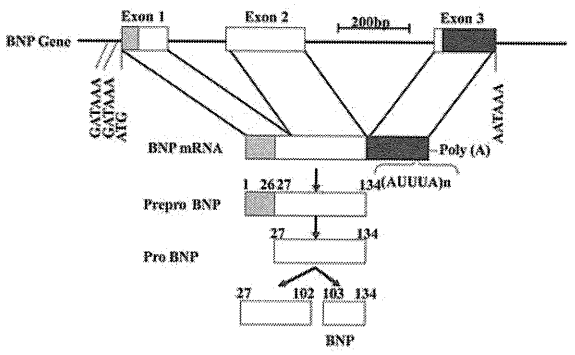


**Figure 1.** Structure of human BNP gene and biosynthesis of human BNP.

**Table I.** Comparison of BNP and ANP

| | BNP | ANP |
|---|---|---|
| Structure | Divergent | Conserved |
| Storage Form | BNP, γ-BNP (ProBNP) | γ-ANP (ProANP) |
| Circulating Form | BNP, γ-BNP (ProBNP) | α-ANP |
| Site of Production | Ventricle > Atrium | Atrium > Ventricle |
| Secretagogue | Ventricular Load | Atrial Load |
| Plasma Level (normal) | 0.9 fmol/mL | 6.4 fmol/mL |
| Increase (Heart Failure) | X 1000 | X 100 |
| Induction | Rapid | Slow |
| Metabolic Clearance | Slow | Rapid |
| Receptor Selectivity | Long-Acting | Short-Acting |
| ANP-A Receptor | ++- +++ | +++ |
| ANP-B Receptor | + | + |
| Clearance Receptor | + | +++ |

**Table II.** What is the Functional Molecule ?

| Diabetes Mellitus | Heart Failure |
|---|---|
| Insulin | BNP |
| C-peptide | N-Terminal pro BNP |
| Proinsulin | ProBNP |

BNP is a cardiac hormone secreted mainly from human ventricle.

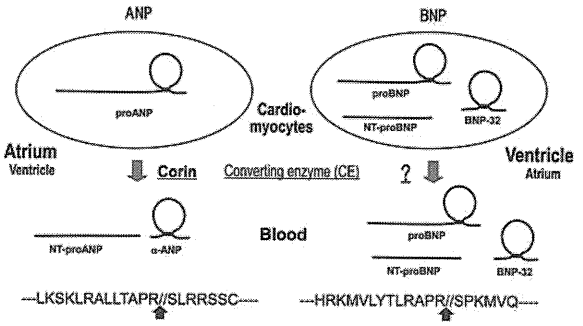


**Figure 2.** Proteolytic processing of proANP and proBNP. Even in healthy subjects, proBNP, BNP-32 and NT-proBNP are present in plasma. In the case of ANP, α-ANP and NT-proANP are main species in plasma of normal subjects, while pro-ANP and β-ANP appear in plasma of HF patients. ProANP is specifically cleaved by corin when secreted from cardiac atrium. Although proBNP-CE in cardiac atrium and ventricle remains unidentified, furin is recognized as a most promising candidate.

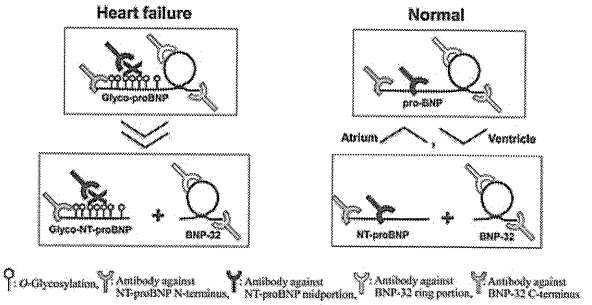


**Figure 3.** Major BNP species in HF patients and normal subjects. In normal subjects, BNP-32 and NT-proBNP are major species, and a proBNP/BNP-32 ratio is high in ventricle and low in atrium. If O-glycosylation is augmented in HF patients and proBNP-CE is furin, Glyco-proBNP should be a major species in heart tissue as well as in blood due to O-glycosylation-induced inhibition of proteolytic processing. The O-glycosylation also interferes antibody binding in the NT-proBNP assay, but not in the BNP-32 assay.

ity with deglycosylation treatment.[10] Collectively, plasma immunoreactive (IR-) BNP species are more complex than thought, and the output from diagnostic kits is a summation of products of the concentration and cross-reactivity of each BNP species shown in Figure 3.

*1) HF may regulate the molecular composition of BNP species in plasma.* proBNP/BNP-32 (high molecular mass IR-BNP/low molecular mass IR-BNP) ratios estimated by gel filtration HPLC were reported to distribute widely depending on the status of HF.[9] This ratio is notably higher in HF patients caused by ventricular overload than atrial overload as well as in those with decompensated HF, and it decreases after treatment. Based on the higher proBNP/BNP-32 ratio in ventricle than in the atrium, the relative contribution of BNP secreted from the ventricle and the atrium is deduced to be a major factor regulating the proBNP/BNP-32 ratio in plasma.

Another key regulator of the proBNP/BNP-32 ratio is a converting enzyme (CE). Furin is a most promising candidate for the proBNP-CE, and converts it into BNP-32 and NT-proBNP *in vitro*.[11,12] One possible explanation for the higher proBNP/BNP-32 ratio in the plasma of HF patients is an imbalance between the expression levels of BNP and CE; less CE leaves more proBNP. On the other hand, a recent report has shown that O-glycosylation at Thr71 impairs cleavage after Arg76 by furin.[12] Glyco-proBNP levels, but not proBNP levels, are elevated in the plasma of HF, suggesting that HF-induced O-glycosylation increases the plasma Glyco-proBNP level as a result.[6,13] Identification of BNP-CEs is a prerequisite for understanding the relation between plasma BNP species and the status of HF. Taking these findings together, concentrations of plasma BNP species vary depending on overloading on the atrium or ventricle, the severity of HF and so forth, which probably alter the degree of O-glycosylation and expression levels of BNP-CEs along with increasing expression of BNP. Inversely, measurements of individual BNP species in plasma are expected to provide more clues to evaluating pathophysiological conditions of heart disease.